ORIGINAL ARTICLE

MicrobiologyOpen WILEY

A hunt for *OM45* synthetic petite interactions in *Saccharomyces cerevisiae* reveals a role for Miro GTPase Gem1p in cristae structure maintenance

Antonina Shvetsova | Ali J. Masud | Laura Schneider | Ulrich Bergmann |
Geoffray Monteuuis | Ilkka J. Miinalainen | J. Kalervo Hiltunen |
Alexander J. Kastaniotis

Faculty of Biochemistry and Molecular Medicine and Biocenter Oulu, University of Oulu, Oulu, Finland

Correspondence
Alexander J. Kastaniotis, Faculty of Biochemistry and Molecular Medicine and Biocenter Oulu, University of Oulu, Oulu, Finland.
Email: alexander.kastaniotis@oulu.fi

Present address
Geoffray Monteuuis, Department of Biochemistry and Developmental Biology, University of Helsinki, Helsinki, Finland

Abstract

Om45 is a major protein of the yeast's outer mitochondrial membrane under respiratory conditions. However, the cellular role of the protein has remained obscure. Previously, deletion mutant phenotypes have not been found, and clear amino acid sequence similarities that would allow inferring its functional role are not available. In this work, we describe synthetic petite mutants of *GEM1* and *UGO1* that depend on the presence of *OM45* for respiratory growth, as well as the identification of several multicopy suppressors of the synthetic petite phenotypes. In the analysis of our mutants, we demonstrate that Om45p and Gem1p have a collaborative role in the maintenance of mitochondrial morphology, cristae structure, and mitochondrial DNA maintenance. A group of multicopy suppressors rescuing the synthetic lethal phenotypes of the mutants on non-fermentable carbon sources additionally supports this result. Our results imply that the synthetic petite phenotypes we observed are due to the disturbance of the inner mitochondrial membrane and point to this mitochondrial sub-compartment as the main target of action of Om45p, Ugo1p, and the yeast Miro GTPase Gem1p.

KEYWORDS
cristae organization, *GEM1*, Miro GTPase, mitochondria, mtDNA inheritance, *OM45*, outer and inner mitochondrial membranes, *UGO1*

1 | INTRODUCTION

The outer mitochondrial membrane (OMM) is the cytosol-exposed sub-compartment that serves as an interface between the organelle and the remainder of the cell. It is the first physical barrier of the organelle, restricting access to the mitochondrial intermembrane space to solutes smaller than 5 kDa (Mannella, 1992; Vander Heiden et al., 2000). Om45p in the yeast *Saccharomyces cerevisiae* has been previously recognized as a major OMM protein in respiring yeast cells (Ohlmeier et al., 2004; Yaffe et al., 1989). The change in the expression of Om45p upon a shift from growth on the fermentable carbon source glucose to non-fermentable glycerol is more than a magnitude higher than the general increase of mitochondrial proteins following the diauxic shift (Ohlmeier et al.,

2004). Hence, Om45p is expected to have a role in mitochondrial functions. Surprisingly, an *om45* knockout yeast strain showed no detectable phenotype under numerous conditions investigated (Yaffe et al., 1989). A C-terminally tagged GFP Om45p is commonly used as a mitochondrial marker in studies of mitochondrial morphology and mitophagy (Sesaki and Jensen, 2001; Kanki et al., 2009).

Om45p is a membrane-anchored protein consisting of a short hydrophobic N-terminal transmembrane sequence of 22 amino acids. The remaining bulk of the protein constitutes a water-soluble domain. For a long time, the latter had been described as facing the cytoplasm (Burri et al., 2006; Riezman et al., 1983; Waizenegger et al., 2003; Yaffe et al., 1989). Lauffer et al. first reported evidence for an intermembrane space orientation of the Om45p C-terminus, along with data indicating the association of Om45p with yeast mitochondrial OMM proteins Por1p and Om14p. This high molecular weight complex interacts physically with the components of the IMM: transporters, adenine nucleotides carrier, the prohibitin complex, respiratory chain complexes III and IV, as well as ATP synthase (Lauffer et al., 2012). Evidence presented by both (Song et al., 2014; Wenz et al., 2014) indicates that Om45p insertion into the OMM is also dependent on protein factors and not only on the lipid composition of the OMM, as had been previously suggested.

Here, we describe the results of a screen for mutations interacting negatively with a deletion allele of *OM45*, revealing a role for its gene product in preserving inner mitochondrial membrane morphology. Using a colony color-based synthetic petite screening approach in *S. cerevisiae*, we isolated three mutants that display a respiratory growth defect in the absence of Om45p. We tracked the source of the mutant phenotypes to point mutations to two distinct genes encoding the evolutionarily conserved OMM proteins, Ugo1p and Gem1p. Deletions of the genes encoding these factors have been previously reported to lead to disturbed mitochondrial morphology (Sesaki and Jensen, 2001; Frederick et al., 2004; Coonrod et al., 2007; Abrams et al., 2015). Our data presented here provide evidence for a joint function of Om45p and Gem1p in mitochondrial cristae structure maintenance and dynamics, and a requirement for *OM45* for mitochondrial DNA (mtDNA) maintenance upon inactivation of its genetically interacting partner *GEM1*.

2 | EXPERIMENTAL PROCEDURES

2.1 | *Escherichia coli* strains and growth media

The *E. coli* strain TOP10 was used for plasmid cloning and propagation (Invitrogen, Carlsbad, CA, USA). *Escherichia coli* BL21 (DE3) (Studier and Moffatt, 1986; Studier et al., 1990) was used for protein production for antibody raising. *Escherichia coli* was cultivated on LB media/agar plates (10 g tryptone, 5 g yeast extract, and 10 g NaCl in 1 L) or LB media/agar plates supplemented with ampicillin 100 µg/ml or chloramphenicol 100 µg/ml. Super optimal broth with catabolite

repression (SOC) (2% tryptone, 0.5% yeast extract, 10 mM NaCl, 2.5 mM KCl, 20 mM glucose, 10 mM MgCl$_2$) was used during *E. coli* chemical transformation and electroporation.

2.2 | Plasmids used in this study

For the plasmids used in the study, see Table 1. Plasmid construction was done using standard techniques (Ausubel et al., 1989). All new constructs were sequence-verified.

2.3 | Yeast strains and growth conditions

For yeast strains used in this work see Table 2. All the strains were derivatives of W1536 8B (Kastaniotis et al., 2004; Zhao et al., 1998). Yeast strains were grown in either rich YPD medium (1% yeast extract, 2% peptone and 2% D-glucose), YPG (3% glycerol), synthetic complete (SC), or synthetic complete drop-out media Kaiser mix (Formedium™, Hunstanton, Norfolk, UK or Sigma-Aldrich, St. Louis, MO, USA) SCD (2% D-glucose), SCG (3% glycerol) or SC media lacking one or more nutrients. Media were solidified with 2% Bacto agar [Biokar – (Sigma-Aldrich)]. Glycerol sectoring medium (GSM) was SCG medium supplemented with 0.05% glucose. The glucose supplementation is necessary for the red color development of the W1536 8B strain on glycerol (Kastaniotis et al., 2004).

2.4 | Yeast transformation

Yeast one-step transformation was carried out as described earlier (Chen et al., 1992) with minor modifications. Briefly, yeast cells from 300 µl of overnight culture were sedimented by a short spin in a table centrifuge (10 s, 11,000 *g*). The supernatant was removed and the cells resuspended in 100 µl of the transformation mix [0.17 M lithium acetate, 34% polyethylene glycol 3350 (PEG), 100 mM DTT, 0.3 µg/µl single-stranded salmon or herring sperm DNA (ssDNA), 1 µl plasmid DNA (0.1–2 µg)]. The cells were incubated in the transformation mix for 30 min at 42°C, plated on the appropriate selective medium, and incubated at 30°C for 3–7 days.

Yeast high-efficiency transformation was performed following the method of Gietz and Woods (Daniel Gietz et al., 2002). Yeast cells were reinoculated from an overnight culture to fresh YPD (or appropriate selective medium) to obtain 5×10^6 cells/ml and incubated for 3–5 h in a shaker while completing 2 doublings. Cells were harvested by centrifuging for 5 min × 3000 *g*, washed once with sterile distilled H$_2$O and once with 100 mM lithium acetate. To each 4×10^6 cells 360 µl of the transformation mix [240 µl PEG (50% w/v), 36 µl 1.0 M. lithium acetate 2 µl ssDNA (10 mg/ml), 0.1–10 µg plus H$_2$O to a volume of 34 µl] were added. Afterward, cells were incubated for 50 min at 42°C. Transformed cells were incubated in YPD liquid medium for 2–4 h and plated onto the appropriate selective medium.

TABLE 1 Yeast strains used in this study

Plasmid	References	Yeast marker
pAG32	Goldstein and McCusker (1999)	*HPHMX*
pET 15b	Novagen	*E. coli* expression vector
pET 15bOM45	This study	*E. coli* expression vector
pTSV30A	generated by J. Pringle and M. Longtine, previously described Kastaniotis et al. (2004)	*LEU2*
pTSV30OM45	This study	*LEU2*
pVT100U mtGFP	Westermann et al. (2000)	*URA3*
pYM8	Knop et al. (1999)	*KanMX*
YCp22FZO1	This study	*TRP1*
YCp22UGO1	This study	*TRP1*
YCp22ugo1-1(P189L)	This study	*TRP1*
YCp33ADH1	This study	*URA3*
YCp33ADH1prom	This study	*URA3*
YCp33ADHpromOM45 (own terminator)	This study	*URA3*
YCp33AIM2	This study	*URA3*
YCp33AIM2	This study	*URA3*
YCp33DNM1	This study	*URA3*
YCp33FZO1	This study	*URA3*
YCp33GEM1	This study	*URA3*
YCp33gem1-1 (R103K))	This study	*URA3*
YCp33gem1-2 (S324N)	This study	*URA3*
YCp33MSC1	This study	*URA3*
YCp33OM45	This study	*URA3*
YCp33OM451GFP	This study	*URA3*
YCp33PET54	This study	*URA3*
YCp33PET9	This study	*URA3*
YCp33PRP3	This study	*URA3*
YCp33RPL27b	This study	*URA3*
YCp33RTT109	This study	*URA3*
YCp33SHY1	This study	*URA3*
YCp33TIM44	This study	*URA3*
YCp33UGO1	This study	*URA3*
YCp33YGR111	This study	*URA3*
YCp33YOR228c	This study	*URA3*
YCplac111	Gietz & Sugino (1988)	*LEU2*
YCplac22	Gietz & Sugino (1988)	*LEU2*
YCplac33	Gietz & Sugino (1988)	*URA3*
YEp112FZO1	This study	*TRP1*
YEp112OM45	This study	*TRP1*
YEp112UGO1	This study	*TRP1*
YEp112ugo1-1 (P189L)	This study	*TRP1*
YEp181OM45-proA	This study	*URA3*
YEp195ADH1promOM45	This study	*URA3*
YEp195AIM2	This study	*URA3*
YEp195AIM2	This study	*URA3*
YEp195DNM1	This study	*URA3*

TABLE 1 (Continued)

Plasmid	References	Yeast marker
YEp195*FZO1*	This study	*URA3*
YEp195*FZO1*	This study	*URA3*
YEp195*GEM1*	This study	*URA3*
YEp195*OM45*	This study	*URA3*
YEp195OM45GFP	This study	*URA3*
YEp195*OM45-GFP*	This study	*URA3*
YEp195*PET54*	This study	*URA3*
YEp195*PRP3*	This study	*URA3*
YEp195*RTT109*	This study	*URA3*
YEp195*SHY1*	This study	*URA3*
YEp195*TIM44*	This study	*URA3*
YEp352(CTA1)OM45	This study	*URA3*
YEplac112	Gietz & Sugino (1988)	*TRP1*
YEplac181	Gietz & Sugino (1988)	*LEU2*
YEp*lac*195	Gietz & Sugino (1988)	*URA3*

TABLE 2 Yeast strains used in this study

Name	Genotype	Reference of the source
W1536 5B/8B	*MAT**a*** (5B)/*MATα* (8B), *ade2Δ*, *ade3Δ*, *can1-100*, *his3-1115*, *leu2-3112*, *trp1-1,ura3-1*	Kastaniotis et al. (2004)
W 1536 8B Δ*om45*	MAT α *ade2Δ*, *ade3Δ*, *can1-100*, *his3-1115*, *leu2-3112*, *trp1-1*, *ura3-1*, *yil136w::KanMX4*	This study
W 1536 8B Δ*gem1*	MAT α *ade2Δ*, *ade3Δ*, *can1-100*, *his3-1115*, *leu2-3112*, *trp1-1*, *ura3-1*, *yal048c::HPHMX*	This study
W 1536 8B Δ*gem1Δom45*	MAT α *ade2Δ*, *ade3Δ*, *can1-100*, *his3-1115*, *leu2-3112*, *trp1-1*, *ura3-1*, *yil136w::KanMX4*, *yal048c::HPHMX*	This study
W1536 8B Δ*om45* Δ*ugo1*	MAT α *ade2Δ*, *ade3Δ*, *can1-100*, *his3-1115*, *leu2-3112*, *trp1-1*, *ura3-1*, *yil136w::KanMX4*, *Δydr470c::HPH MX4*	This study
W1536 8B Δ*psd2*	MAT α *ade2Δ*, *ade3Δ*, *can1-100*, *his3-1115*, *leu2-3112*, *trp1-1*, *ura3-1;psd2::ClonNat*	This study
W1536 8B Δ*psd1Δpsd2*	MAT α *ade2Δ*, *ade3Δ*, *can1-100*, *his3-1115*, *leu2-3112*, *trp1-1*, *ura3-1;* *psd2::ClonNat; ynl169c::HPH MX*	This study
W 1536 8B Δ*gem1Δom45Δpsd2*	MAT α *ade2Δ*, *ade3Δ*, *can1-100*, *his3-1115*, *leu2-3112*, *trp1-1*, *ura3-1*, *yil136w::KanMX4*, *yal048c::HPHMX*, *psd2::ClonNat*	This study
W 1536 8B Δ*om45* Δ*psd2*	MAT α *ade2Δ*, *ade3Δ*, *can1-100*, *his3-1115*, *leu2-3112*, *trp1-1*, *ura3-1*, *yil136w::KanMX4*, *psd2::ClonNat*	This study
W 1536 8B Δ*gem1* Δ*psd2*	MAT α *ade2Δ*, *ade3Δ*, *can1-100*, *his3-1115*, *leu2-3112*, *trp1-1*, *ura3-1*, *yal048c::HPHMX*, *psd2::ClonNat*	This study
W1536 5B *rho*^{0} (Δ*etr1*)	*MAT* α *ade2Δ*, *ade3Δ*, *can1-100*, *his3-1115*, *leu2-3112*, *trp1-1*, *ura3-1*, *rho*0, *etr1Δ*	Kursu et al. (2013)

2.5 | PCR-mediated gene replacement

All yeast knockout strains were created by PCR-targeting with short flanking homology (PCR-mediated gene replacement). The homologous ends of the transferring DNA were introduced by primers with a short region (25 bases) homologous to the knockout cassette (KANMX or HPHMX) and a region (40–45 bases) homologous to the gene to be replaced (5′ or 3′ to the stop and start codons of the ORF of the gene) (Goldstein and McCusker, 1999; Knop et al., 1999). The resulting PCR product, therefore, consists of the KANMX (or HPHMX) dominant antibiotic resistance gene and the target gene homologous regions. This DNA product was introduced to the yeast

cell by high-efficiency transformation. KANMX (or HPHMX) integrates at the target locus, resulting in geneticin (or hygromycin) resistant transformants. The success of the knockout procedure was verified by PCR.

2.6 | Droplet digital PCR (ddPCR)

Yeast genomic DNA (gDNA) from each sample was isolated using the method described previously (Hoffman and Winston, 1987). The concentration and purity of the DNA were determined using the NanoDrop 1000 spectrophotometer (Thermo Fisher Scientific Inc., Waltham, MA, USA) and restriction digested with the Sac1-HF (New England BioLabs Inc., Ipswich, MA, USA). A final concentration of 0.1 ng digested DNA was used for the Droplet Digital Polymerase Chain Reaction (ddPCR). Unless otherwise stated, all the instruments, software, consumables, primers, and probes related to the ddPCR experiments were purchased from Bio-Rad Inc., Hercules, CA, USA. The mtDNA encoded cytochrome c oxidase subunit 3 (COX3) (SGD ID S000007283) gene, which encodes one of the three mtDNA subunits of complex IV of the mitochondrial electron transport chain, was used as a marker gene for the yeast mtDNA genome maintenance. A ddPCR reaction probing the nuclear-encoded gene ACT1 (SGD ID S000001855) (encoding actin) was used as a standard. COX3 and actin gene-specific primers were labeled with HEX and FAM probes respectively. The COX3 primers sequences were: forward primer 5′- CATTCAGCTATGAGTCCTG-3′, reverse primer 5′-CCTGCGATTAAGGCATG-3′ and Probe sequence: 6HEX 5′-AGG TGCATGTTGACCACCCGTAGG-3′-Iowa Black FQ. The ACT1 primer sequences were: forward primer 5′-CAAACCGCTGCTCAAT-3′, reverse primer 5′-TACCTGGGAACATGGTG-3′, and the probe 6FAM-5′-TGGTAACGAAAGATTCAGAGCCCCAGAAG-3′-Iowa Black FQ. A T100™ Thermal Cycler and the QX 200™ droplet reader were used and a count of the positive and negative droplets (events) utilizing the HEX/FAM channels was performed. The wells displaying ≥15,000 events were chosen for the analysis. QuantaSoft 1.7.4 software was used to analyze the copy number variation (CNV). The reference gene was ACT1 (one copy/haploid cell). CNV was expressed as copies/cell. Three biological replicates were performed in the analysis.

2.7 | Mutagenesis and sectoring screen

Ethyl methanesulfonate (EMS) mutagenesis was performed as described previously (Amberg et al., 2005). Yeast cultures were grown to an early stationary phase in SC selective medium supplemented with 2% glucose. Two separate 1 ml samples (one as a control) were pelleted in a table centrifuge (10 s, 5000 g). The obtained pellets were washed once with distilled sterile water and resuspended in 0.1 M sodium phosphate buffer (pH 7.0). 30 µl of EMS were added to one of the two tubes and mixed by vortexing. Both tubes were incubated for 50 min at 30°C. Cells were pelleted, resuspended in 200 µl of 5% sodium thiosulfate, transferred to fresh tubes, and

washed twice with 200 µl of 5% sodium thiosulfate, resuspended in 1 ml of sterile water, and plated. 1:10–1:10,000 dilutions from both the sample and the control (the cells incubated without EMS) were prepared for later calculation of the killing rate, which ranged between 50–80%. Petri dishes with cells plated on GSM medium were incubated at 30°C for 10–15 days. The sectoring screen was performed manually as described earlier (Kastaniotis et al., 2004; Kursu et al., 2013).

2.8 | Cloning of the synthetic mutations

Upon loss of the OM45 containing plasmid, it was not possible to complement the synthetic petite mutants with any plasmid encoding the intact copies of OM45 or the mutated genes (our observation). For this reason, cloning by complementation had to be accomplished via two plasmid shuffles. First, the synthetic petite mutants carrying the pTSV30OM45 plasmid were transformed with multicopy YEp112OM45 (TRP1 selective marker). Sectoring colonies obtained after the transformation were streaked out on SCG-TRP media containing 0.05% glucose. The white colonies collected from this restreaking were further tested on SCD-LEU plates to confirm the loss of the pTSV30OM45 plasmid. The TRP1 marker allowed us to perform a counterselection against the OM45 plasmid using 5-fluoroanthranilic acid (5-FAA) in the following step. For cloning of the mutations by complementation two multicopy libraries were used. pRS426-based (referred in the text as HeAl) (Kastaniotis et al., 2004) was made in the Heitman laboratory by Clara Alarcon and contains yeast genomic sequences inserted in the Sal1 site of the vector and Lacroute library constructed by F. Lacroute in pFL44L (2µ plasmid with a URA3 marker) (Bonneaud et al., 1991) with genomic DNA of strain FL100 (Harington et al., 1993).

Mutant strains carrying YEp112OM45 were grown overnight on SCD-TRP media, transformed with the Lacroute or the HeAl library according to the high-efficiency lithium acetate/SS-DNA/PEG protocol (Gietz & Woods, 2002), and plated on SCG-URA plates containing 250 mg/L 5-FAA, low tryptophan (10 mg/L) and 0.05% glucose. Glucose was added in this case to enhance the recovery of library transformants. The used concentration is low enough to allow for efficient selection of the respiratory competent colonies.

2.9 | Test for petite colonies generation rate

Strains from SCG plates grown overnight in liquid medium (YPD) were plated onto SCD to yield approximately 50–100 colonies per plate. After 7 days of incubation at 30°C, the colonies were replica plated onto YPD and SCG and incubated for 3–7 days at 30°C. The number of colonies on corresponding SCG (respiratory competent) and YPD (total number of colonies) plates were determined. The number of the petite colonies = number of colonies on YPD plate minus number of colonies on SCG plate.

2.10 | Construction of His6-Om45p, protein expression, purification, and antibody production

DNA encoding the soluble domain of Om45p without the first 22 amino acids (predicted N-terminal transmembrane domain) was cloned onto the expression vector pET15b (Novagen-Addgene, Cambridge, MA, USA) and expressed in *E. coli* BL21 (DE3). The expressed chimeric protein containing a His6 tag on its N-terminus, a thrombin cleavage site, and N-terminally truncated Om45p was affinity purified with Ni^{2+} chelating Sepharose (GE Healthcare, Piscataway, NJ, USA), concentrated 10 times with a Millipore Amicon Ultra-15 10000 NMWL concentrator (Carrigtwohill, Cork, Ireland) in a table centrifuge at 4°C and subjected to anion-exchange chromatography in Fractogel EMD DEAE (M) (Merck KGaA, Darmstadt, Germany), in a 10 × 150 mm column (20 mM Tris/HCl pH 7.4, linear gradient elution with NaCl from 50 to 200 mM at the flow rate 1 ml/min in 25 min). The purity of the peak fractions was controlled by SDS-PAGE and mass spectrometry. Peak fractions were concentrated to 1.69 mg of protein per ml. 500 µl of the protein were used for the generation of polyclonal antisera fin two rabbits by Davids Biotechnologie (Regensburg, Germany).

2.11 | Fluorescence microscopy

Fluorescence microscopy was performed with either live or fixed cells using a Zeiss LSM700 confocal fluorescence microscope at 100x magnification. Mitochondria were visualized as described previously (Westermann and Neupert, 2000) with pYX142*mtGFP*, pVT100U*mtGFP*, or using MitoTracker®Red CMX-ROS (Molecular Probes, Eugene, OR, USA). DAPI (Thermo Scientific, Rockford, IL, USA) staining of mtDNA in methanol-fixed cells was performed as described previously (Jones and Fangman, 1992).

2.11.1 | Yeast cell fixation

For fixation, yeast cells were incubated in the growth media containing formaldehyde 4.4% (v/v) final concentration for 30 min at 30°C under shaking, then washed with 1.2 M sorbitol in 0.1 M potassium phosphate (KP_i) buffer (pH 6.5), harvested at 700 g for 1 min and stored at 4°C (Lee et al., 1996).

2.12 | Transmission electron microscopy

Transmission electron microscopy was performed according to the Tokuyasu method for yeast described previously (Griffith et al., 2008). Cells were fixed in 2% paraformaldehyde, 0.2% glutaraldehyde in 0.1 M PHEM buffer (60 mM PIPES, 25 mM HEPES, 10 mM EGTA, 2 mM MgCl2, pH 6.9) at room temperature for 3 h. Cells were washed with 0.1 M PHEM buffer, resuspended in 1% periodic acid in 0.1 M PHEM buffer, and incubated at room temperature for 1 h.

After washing in 0.1 M PHEM buffer, cells were infiltrated with 12% gelatin dissolved in 0.1 M PHEM buffer at 37°C for 10 min. After solidification at 4°C, small gelatin blocks were immersed in 2.3 M sucrose and frozen in liquid nitrogen. Ultrathin (75 nm) sections were cut at −100°C using UC7 ultramicrotome with cryo attachment (Leica Microsystems) and picked up on grids with a drop of 1% methylcellulose, 1.1 M sucrose mixture in PHEM buffer. Sections on a grid were contrasted with 2% neutral uranyl acetate for 5 min, embedded in 2% methylcellulose, 0.4% uranyl acetate mixture, and examined using Tecnai G2 Spirit transmission electron microscope (FEI Europe, Eindhoven, Netherlands). Images were captured by a Quemesa CCD camera and analyzed using iTEM software (Olympus Soft Imaging Solutions, Münster, Germany). Yeast cell fixations and electron microscopy were performed by the staff of the Biocenter Oulu Electron microscopy core facility.

2.13 | Lipid analysis

2.13.1 | Preparation of the cells for lipid extraction

To prevent DNA loss during culture growth, yeast cell lawns were prepared on SCG plates supplemented with 2 mM ethanolamine (Etn) (Sigma-Aldrich), by incubation at 30°C for 4 days. The Etn supplementation was necessary since the negative control W1536 8B Δ*psd1*Δ*psd2* strain is an auxotroph for Etn. The cells were scraped with 2 × 2 ml SCG containing Etn (or SCD containing Etn) media, inoculated in 400 ml SCG containing Etn (or SCD containing Etn) to OD_{595} 0.4, and grown for 43 h (or 15 h in case of SCD containing Etn).

For the phospholipidome analysis yeast cells were harvested from a 400 ml growth culture by centrifugation. The cell mass was adjusted to 1 g wet weight, washed with sterile water. Cells were pelleted by centrifugation (5 min, 3000 *g*), the pellets were frozen and stored at −70°C until lipid isolation.

2.14 | Mitochondrial isolation for lipid extraction

Highly purified mitochondria were prepared as described before by Meisinger et al. (2000). Briefly, yeast cultures grown as described above were harvested by centrifugation (Beckman J-6-Mi) for 35 min at 5000 *g*, washed with deionized water, and incubated for 20 min in DTT buffer [100 mM Tris/H_2SO_4 (pH 9.4), 10 mM DTT], 2 ml/g of wet cells, washed with zymolyase buffer [1.2 M sorbitol, 20 mM potassium phosphate buffer (pH 7.4)] and then digested with zymolyase 20T (5 mg/g of wet cells) in zymolyase buffer for 30 min. Spheroplasts were lysed in a Teflon potter (500 rpm) using 6.5 ml of homogenization buffer [(0.6 M sorbitol, 10 mM Tris/HCl, pH 7.4, 1 mM EDTA, 1 mM phenylmethylsulfonyl fluoride (PMSF), 0.2% (w/v)] per gram of wet cells. The homogenate was centrifuged at 1500 *g* for 5 min and the supernatant was further cleared by centrifugation at 3000 *g* for 5 min. The crude mitochondria from the supernatant were collected by centrifugation in the SS-34 rotor at

12,000 **g** for 15 min. The mitochondrial pellet was resuspended in cold SEM buffer (250 mM sucrose, 1 mM EDTA, 10 mM Mops, pH 7.2), manually homogenized in a small Teflon potter with 20 strokes, and centrifuged at 12,000 **g** for 15 min. The pellets were resuspended in 5 ml of cold SEM buffer, applied to the sucrose gradient, and ultracentrifuged at 100,000 **g** for 30 min at 4°C. Mitochondria were collected with a syringe needle from the interface between the 32 and 64% sucrose layers. Mitochondria were washed with SEM buffer, weighed, flash-frozen in liquid nitrogen in 200 μl of the SEM buffer, and stored at −70°C.

The yeast samples for the lipid analysis were grown on synthetic complete media containing either glucose or glycerol, supplemented with 2 mM Etn.

2.14.1 | Lipid extraction

Frozen cells (1 g) were thawed at room temperature and subjected to ethanol extraction (95% ethanol, 4 ml) in acid pre-washed glass tubes with a Teflon cover (Pyrex England) at 22°C for 1 h under constant shaking (Vari-Mix, Barnstead/Thermolyne, Ashville, NC, USA). The standard lipids (1,2-diheptadecanoyl-sn-glycerol-3-phosphatidylethanolamine m/z (–) 718.5387; 1,2-diheptadecanoyl-sn-glycerol-3-phosphatidyl-L-serine sodium salt m/z (–) 762.5292; 1,1,2,2-tetramyristol-cardiolipin (ammonium salt) m/z (–) 1239.841; L-α-lysophosphatidylcholine-palmitoyl-D$_3$ (methyl-D$_3$) m/z (–) 557.36, each 0.2 μg/sample, were added to control the efficiency of the extraction. After 5 min spinning at 4100 g the supernatant was collected in a glass evaporation tube (vial no.1; Verex™. Phenomenex®, Torrance, CA, USA) and evaporated in a speed vac (ThermoElectron, SPD 2010, Ashville, NC, USA) at 45°C under vacuum. The pellets were further extracted twice for 20 min with 2 ml chloroform: methanol (2:1 v:v), centrifuged at 4000 **g** for 5 min after each extraction, and finally extracted twice in acidic solvent (20 min with 2 ml of chloroform: methanol: HCl (124:65:1 v:v:v) followed by centrifugation at 4000 **g** for 5 min after the acidity was adjusted to pH 4.0 with 0.5 M NaOH. Extracts from all steps were redissolved in 1 ml CHCl$_3$: methanol (2:1 v:v), combined and washed with 1 ml 0.9% NaCl of pH 3.0 (Christie, 2003).

Experiments with the lipids obtained from whole cells were performed in the following replicates: three independent experimental repeats were performed for each yeast strain; one to three independent repeats were taken from each sample culture. Two to three independent mass spectrometric measurements were performed from each lipid extraction. Overall, 13 measurements per yeast strain were performed for the determination of the phospholipid content in whole cells and six for the analysis of the mitochondrial phospholipidome.

2.14.2 | LC-MS analysis

The separation of the phospholipids was performed on a UPLC® HSS T3 1.8 μm column (2.1 × 100 mm) at 55°C using an ultra-performance LC system (Waters Acquity™, Milford, MA, USA). The binary gradient was made with A: 10 mM ammonium acetate in acetonitrile and deionized water (60:40); B: 10 mM ammonium acetate in isopropanol/acetonitrile (90:10). The column was eluted at 0.35 ml/min with a linear change from 60 to 100% B over 15 min.

Eluted lipids were analyzed by positive and negative electrospray ionization in separate runs on a Synapt G-2 Quadrupole/time of flight mass spectrometer in MSE mode with lock mass correction over a mass range from 100 to 1500 Da.

Data were processed with Mass Lynx and its Marker Lynx option to obtain automatic quantification of large data sets. The ion counts were normalized to internal standards; lipids were identified by their accurate masses, MS/MS fragmentation, and their chromatographic behavior. The analysis was focused on the most abundant (C 34:2, C 34:1, C 32:2 and C 32:1) phosphatidylserine (PS), phosphatidylethanolamine (PE), phosphatidylcholine (PC) and cardiolipin (CL) (CL 64:4; CL 66:4; CL 68:4; CL 70:4 and CL 72:4) species.

2.15 | Protein analysis

2.15.1 | Protein extraction for western blot analysis

Proteins were extracted from the cultured yeast cells or directly from the plate lawns as described previously by Platta et al. (2004). In brief, cells were harvested by centrifugation, washed with sterile water. 30 mg of cell pellets and mixed with 15 μl of 1 M potassium phosphate buffer, pH 7.4 and 100 μL of trichloroacetic acid were incubated for 30 min at −70°C, thawed, and pelleted. Proteins were further precipitated in 500 μl of ice-cold 80% acetone, pelleted, re-dissolved in 60 μl of 1% SDS/0.1 M NaOH and 20 μl of 4 × SDS loading buffer [500 mM Tris/Cl (pH 6.8), 10% SDS, 30% glycerol, bromphenol blue, 10% β-mercaptoethanol], heated 5 min at 95°C.

2.15.2 | SDS-PAGE and western blot analysis

Proteins were analyzed by SDS-PAGE (12%) (Laemmli, 1970), stained with Coomassie brilliant blue, or subjected to western blotting using nitrocellulose membranes (Bio-Rad) and the enhanced chemiluminescence system (Bio-Rad).

3 | RESULTS

3.1 | Synthetic petite screen

It has been previously reported that Om45p is not essential for yeast growth or mitochondrial functions (Yaffe et al., 1989). Our W1536 8B *om45* deletion strain, a derivative of W303, grew equally well as the corresponding wild-type strain under the growth conditions investigated (Figure A1). We hypothesized that the absence of any growth phenotype for the major protein of the OMM may be due

to the presence of (a) protein(s) with redundant functions. This possibility was addressed in a screen for synthetic petite mutants (SPM) (Kursu et al., 2013) (Figure 1a). W1536 5B/8B strains carrying an _ade2_, _ade3_ double deletion, as well as _leu2_, _ura3_, and _trp1_ marker mutations are deleted for _om45_ (Δ_om45_). When transformed with the pTSV30_OM45_ plasmid carrying _OM45_ and _ADE3_ genes (as well as the _LEU2_ gene as a transformation selection marker), the cells become genotypically Δ_ade2_ and develop the characteristic red colony color phenotype. Without selection for the plasmid, it is lost at high frequency, resulting in a "sectored" colony color appearance. The cells are exposed to the mutagen ethyl methanesulfonate (EMS) and plated on media containing only a non-fermentable carbon source. Synthetic petite mutants are identified by their inability to lose the _OM45_ plasmid on non-fermentable media, which can be monitored by the formation of completely red, non-sectoring colonies on synthetic complete glycerol (SCG) media. The ability to lose the _OM45_ plasmid on synthetic complete dextrose (glucose) (SCD) media indicates that the mutation only affects mitochondrial function, but not respiratory growth. The screen was designed to identify mutations that in absence of _OM45_ would lead to a synthetic growth defect specifically on non-fermentable media containing glycerol, but not on fermentable media containing glucose. We screened over 50,000 colonies and obtained three stable synthetic petite mutants in a Δ_om45_ strain background that were dependent on an _OM45_ plasmid for growth on SCG after chemical mutagenesis. These mutants readily lost the _OM45_ plasmid on SCD, upon which they became respiratory deficient, and were viable on fermentable carbon sources in absence of _OM45_ (Figure 1b and c). Upon loss of the _OM45_-containing plasmid, it was not possible to complement the synthetic petite mutants (SPMs) with any plasmid encoding the intact copies of _OM45_. Hence, all the complementation experiments and cloning of the mutations by library complementation were done via plasmid shuffle. The obtained synthetic petite mutants were recessive, as diploids of the Δ_om45_ parentals with the SPMs are respiratory competent in absence of the _OM45_ plasmid.

3.2 | Synthetic mutations in the _GEM1_ and _UGO1_ genes

The gene alleles with acquired point mutations in the three synthetic petite mutant yeast lines were identified by cloning based on genomic DNA library complementation. For this purpose, two yeast multicopy genomic DNA libraries: HeAl (Kastaniotis et al., 2004) and Lacroute (Bonneaud et al., 1991; Harington et al., 1993) were used for transformation of the synthetic petite mutants carrying the YEp112_OM45_ plasmid. The latter construct carries a _TRP1_ marker gene that can be selected against on 5′ fluoroanthranilic acid (5′FAA)-containing media. From about 50,000 independent transformants able to grow on selective media supplemented with glycerol upon loss of the YEp112_OM45_ plasmid, several independent clones containing _OM45_ were isolated during our library complementation screen, confirming the good quality of the libraries and

the validity of the cloning strategy. We tracked the cause of the mutant phenotype of the synthetic petite strains to point mutations in two distinct genes encoding OMM proteins Ugo1p, a participant in the mitochondrial fusion machinery (Sesaki and Jensen, 2001), and Gem1p, the mitochondrial Rho (Miro) GTPase (Frederick et al., 2004) (Figure 1d and e). Single copy plasmids carrying wild-type alleles of these plasmids complemented, as well as the original multicopy (2μ) library plasmids. Sequencing of the mutant alleles revealed a transition mutation in _ugo1_(c.566C>T), translating to p.P189L in the mutant Ugo1 protein. This mutation is located in a segment of the Ugo1p amino acid sequence that is exposed to the intermembrane space (IMS) (Hoppins et al., 2009). We mapped the _gem1-1_ (c.308G>A/ p.R103K) mutation to the first GTPase domain of Gem1p and _gem1-2_ (c.971G>A/p.S324N) to the region between the two EF-hand domains of the protein (Frederick et al., 2004) (Figure 1d and e). The _OM45_ genetic interactions with both _GEM1_ and _UGO1_ found in our screen are consistent with high throughput yeast synthetic lethality data reported before (Hoppins et al., 2011). The Gem1 and Ugo1 proteins have previously been shown to play a role in yeast mitochondrial morphology maintenance (Frederick et al., 2004; Sesaki and Jensen, 2004).

3.3 | Mitochondrial morphology defects in synthetic petite mutants devoid of _OM45_ plasmid

In addition to the growth defects, SPM demonstrated changes in mitochondrial structure. We examined mitochondrial morphology in SPMs in the presence and absence of an _OM45_ plasmid (Figure 2). Mitochondria of the _ugo1(P189L)_ SPM strain grown on glucose media displayed many fragmented, collapsed mitochondria close to each other, nonetheless apparently unable to fuse and form the long tubular structures that can be found in the WT control. The presence of the plasmid-borne copy of _OM45_ slightly ameliorated the phenotype and some tubular-like mitochondria were present. SPMs of _gem1(R103K)_ and _gem1(S324N)_ (not shown) also contained many fragmented and collapsed mitochondria. Some tubular mitochondrial structures were present in these mutant cells, although the diameter of such tubules was irregular, they appeared collapsed and reminiscent of a "beads on a string" arrangement. The appearance of mitochondria in the SPMs clearly differs from the morphology observed in rho^0 cells, which maintain a tubular structure (Sesaki & Jensen, 2001). Thus, observed changes in SPM mitochondrial morphology cannot be explained as a consequence of mtDNA loss. The presence of plasmid-borne _OM45_ improved the SPM phenotype, resulting in mitochondria with a more tubular structure and more regular in diameter (Figures 2, 3).

Electron microscopy analysis of the SPMs with and without the plasmid copy of _OM45_ revealed defects in the folding of the inner mitochondrial membrane (IMM) (Figure 4). The double membranes of mitochondria were clearly observed, but the IMM was completely devoid of regular cristae organization (compare the figure to wild-type examples in Figure A2a–d), was found either
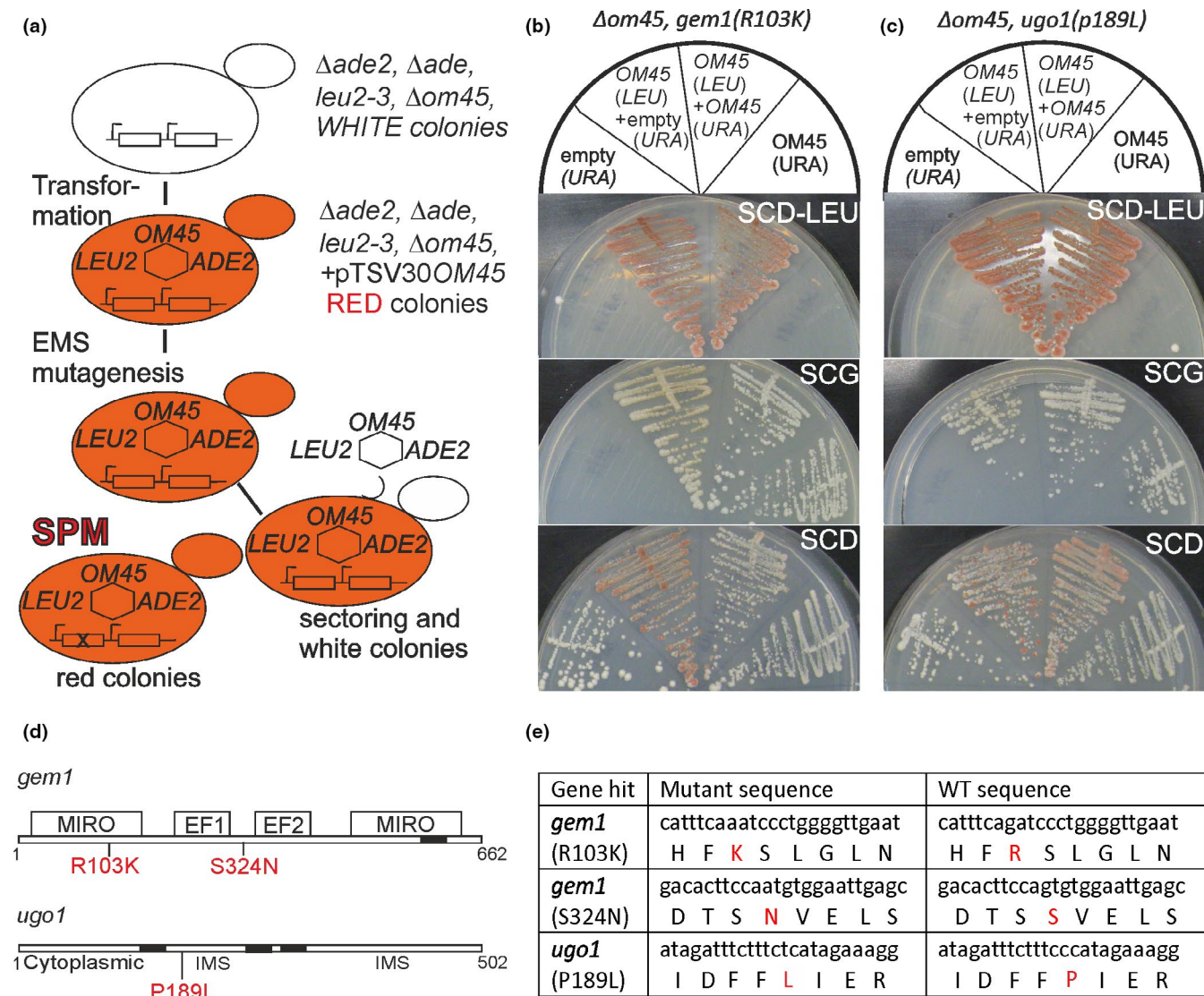
FIGURE 1 Synthetic petite screen in yeast hunting for genetic interactions of OM45. (a) Schematic outline of the screen. See text for further description. SPM synthetic petite mutant. The X symbolizes the mutation in an interacting gene. (b) and (c) Test for a dependence of SPMs on the OM45 plasmid for respiratory growth and demonstration of respiratory deficiency in absence of OM45. (b) The synthetically petite mutant gem1(R103K) and (c) ugo1(P189L) obtained via the genetic screens are respiratory deficient upon loss of the OM45 plasmid. All the complementation studies were done via plasmid shuffle, loss of the original pTSV30OM45 plasmid was monitored via colony sectoring and confirmed by re-streaking on SC-LEU drop-out media supplemented with glucose. Only strains that carry a copy of OM45 on a plasmid are viable on respiratory media (SCG). All strains can grow on media containing the fermentable carbon source glucose (SCD, lowest panel). (d) Schematic representation of the location of the obtained synthetic mutations in the Gem1p and Ugo1p translation products based on published data on Ugo1p (Hoppins et al., 2009) and Gem1p (Frederick et al., 2004) Black boxes designate transmembrane domains (TMDs). MIRO, GTPase domains; EF1/2, EF-hand domains. (e) Nucleotide and amino acid sequences of obtained synthetic petite mutations. The nucleotide sequence excerpts displaying the gem1(R103K) and gem1(S324N) mutations show nucleotides 301–324 and 961–984 of the GEM1 ORF, respectively. The UGO1 ORF sequence excerpt stretches from 553 to 576. Mutated amino acid residues and corresponding wild-type residues are marked in red

adjacent to the OMM or forming a stretch along the mitochondria approaching the OMM at both ends or displaying small circles and exhibited a multi-layered appearance. In contrast, the cristae organization of W303 strain background cells carrying the Δgem1 mutation alone has been reported to be unaffected (Frederick et al., 2004) and the IMM of W1536 8B Δom45 strain is indistinguishable from wild type under regular growth conditions. The membrane morphology of the SPMs also differs from the membrane defects observed in rho^0 cells, which lack properly formed cristae but do neither exhibit the multi-layered membrane phenotype nor the dramatic clustering that can be observed in SPM mitochondria (Figures A2e–h). These results indicated a synthetic negative effect of om45 and gem1 mutations on IMM structure. The presence of a multicopy OM45-carrying plasmid visibly relieved the severity of the phenotype, largely restoring the classical cristae organization of most mitochondria.
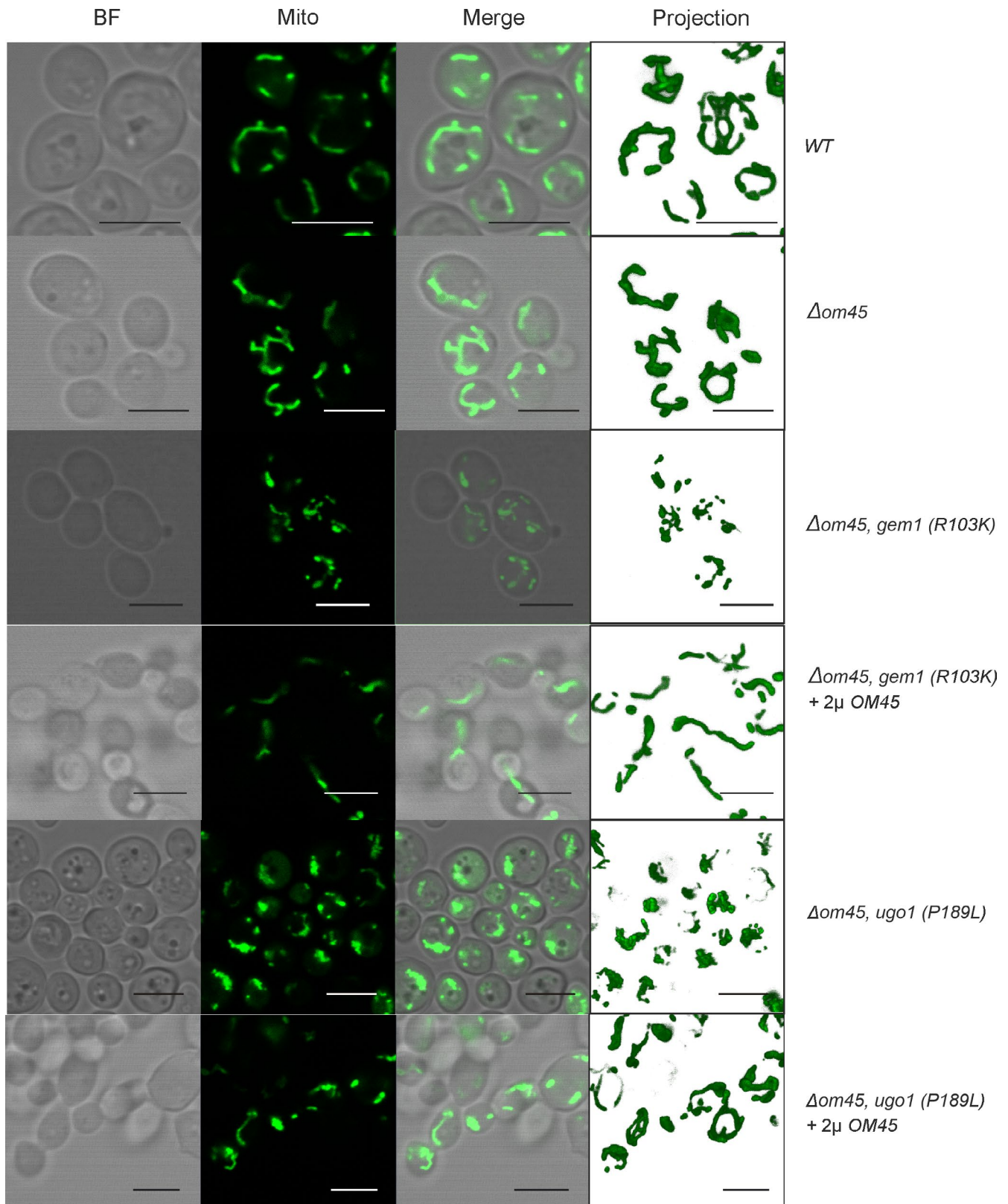
FIGURE 2 Synthetic lethal mutants show mitochondrial morphology defects in the absence of the complementing OM45 plasmid. Yeast cells from wild-type (WT), SPMs, and SPMs with the complementing plasmid were grown in selective liquid synthetic complete medium supplemented with glucose (2%) to mid-log phase, and mitochondria (Mito) were visualized by mitochondria-targeted GFP. The om45 deletion does not visibly affect mitochondrial morphology (second row from the top). The gem1 mutants still maintain some tubular structure but display mitochondrial fragmentation and collapsed structure (rows three and four from the top). This phenotype is exacerbated in the ugo1 SPM, which nearly completely lacks long tubular mitochondria. Mitochondrial morphology of the SPM cells is rescued by the presence of a plasmid-borne copy of OM45, here shown for the Δom45,ugo1(P198L) SPM. BR, brightfield image; Mito, mitochondrially targeted GFP. Projection images of mitochondria were generated using the Zeiss software (see Experimental procedures). Size bar: 5 μm
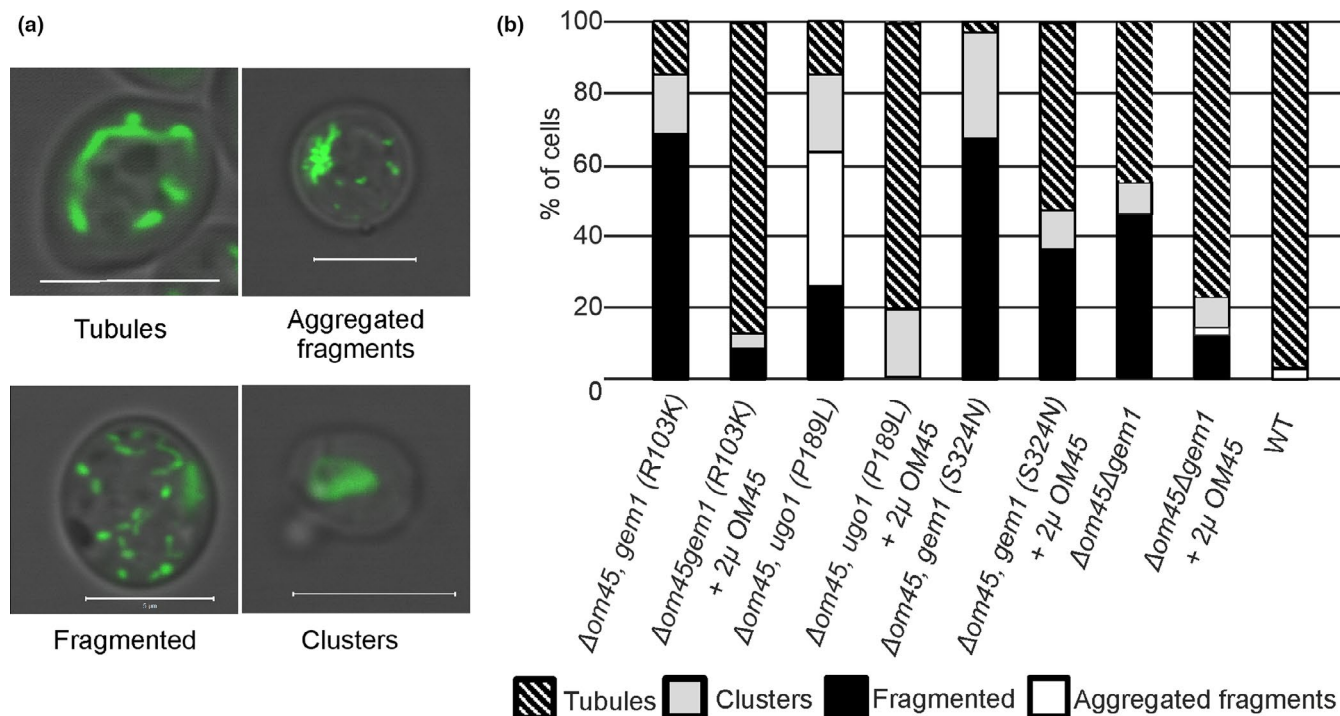
FIGURE 3 Quantitative analysis of mitochondrial morphology types in SPM cells in the absence or presence of complementing OM45. (a) Representative images of morphology types observed in W1536 8B Δgem1Δom45 cells with and without the complementing 2μ OM45 plasmid. Mitochondria were visualized using matrix targeted mtGFP expressed from the pVT100 U mtGFP (URA3) plasmid. Cells were grown overnight in a selective liquid synthetic complete medium supplemented with glucose (2%). (b) Quantification of mitochondrial morphology phenotypes as exemplified in panel A. Shown are % ratios of cells from 2 experimental replicates observing at least 100 cells in each experiment, except for data of mutant Δom45, gem1(R103K) for which results of one set of 100 examined cells are shown

3.4 | Reconstruction of the mutants

To better characterize the SPMs, we performed a tetrad analysis of Δom45/ Δom45-SMP diploids. The dissection pattern of the mutants during the tetrad analysis (Figure A3) did not follow Mendelian segregation. If only one mutation was involved we would expect a clear 2:2 (viable:non-viable) segregation pattern on glycerol. In case two mutations were required to get the respiratory deficient phenotype in the Δom45 background, we would expect: 2:2 for the parental ditype, 4:0 for the non-parental ditype, and 3:1 for the tetratype. There is no scenario following Mendelian genetics that would ever result in a 0:4 (respiratory competent:respiratory deficient) ratio, which we frequently encountered in the tetrad dissection analysis of the *gem1* SPMs. Tetrad analysis of the *ugo1* SPM yielded many 4:0 (respiratory competent:respiratory deficient) and a few 3:1 tetrads, not consistent with a simple relationship between the Δom45 genetic background and the *ugo1* SPM.

In our interpretation, the erratic inheritance pattern of the *gem1* SPMs was caused by disturbed mitochondrial DNA inheritance. Because this feature of our mutants interfered with our attempts to breed out possible background mutations and to investigate or completely rule out the possibility of a complex combination of several nuclear mutations as the root of the non-Mendelian segregation pattern, we reconstructed the mutant genotype in cells that had not been exposed to EMS mutagenesis.

The W1536 8B Δgem1Δom45 double deletion strain was created by introducing the *HPHMX* KO cassette (conferring hygromycin resistance) into the *GEM1* locus the W1536 8B Δom45 strain, thereby removing *GEM1*. None of the single deletion strains (Δgem1 or Δom45) are respiratory deficient (Frederick et al., 2004; Yaffe et al., 1989). The obtained Δgem1Δom45 double deletion strain, in contrast to the *gem1* point mutation SPMs, was initially not respiratory deficient but a very slow grower on glycerol-containing media. The Δom45gem1(R103K) and Δom45gem1(S324N) point mutants were reconstructed by the introduction of the plasmid-borne *gem1(R103K)* and *gem1(S324N)* alleles into the W1536 8B Δgem1Δom45 double deletion strain. The behavior of these three reconstructed strains under different growth conditions was tested (Figure 5a). A plasmid harboring wild-type *GEM1* (YCp33GEM1) completely rescued the growth of the W1536 8B Δgem1Δom45 strain, whereas YCp33gem1(R103K) and YCp33gem1(S324N) rescued the growth only partially, (Figure 5a).

Since the *ugo1* null mutant is respiratory deficient as a result of mtDNA loss after the loss of *UGO1* (Sesaki and Jensen, 2001), reconstruction of the strain was achieved *via* plasmid shuffle. The *UGO1* gene was knocked out in the presence of a plasmid carrying a wild-type *UGO1* allele and the *ugo1* (P189L) allele was then introduced with a second plasmid, selecting against the initial construct carrying the wild-type copy. On the non-fermentable media SCG the growth of the Δom45, Δugo1/ugo1(P189L) reconstructed synthetic

+*OM45* plasmid   **- *OM45* plasmid**

(a) *Δom45 gem1*(R103K)+*OM45*

(b) *Δom45 gem1*(R103K)

(c) *Δom45 gem1*(S324N)+*OM45*

(d) *Δom45 gem1*(S324N)

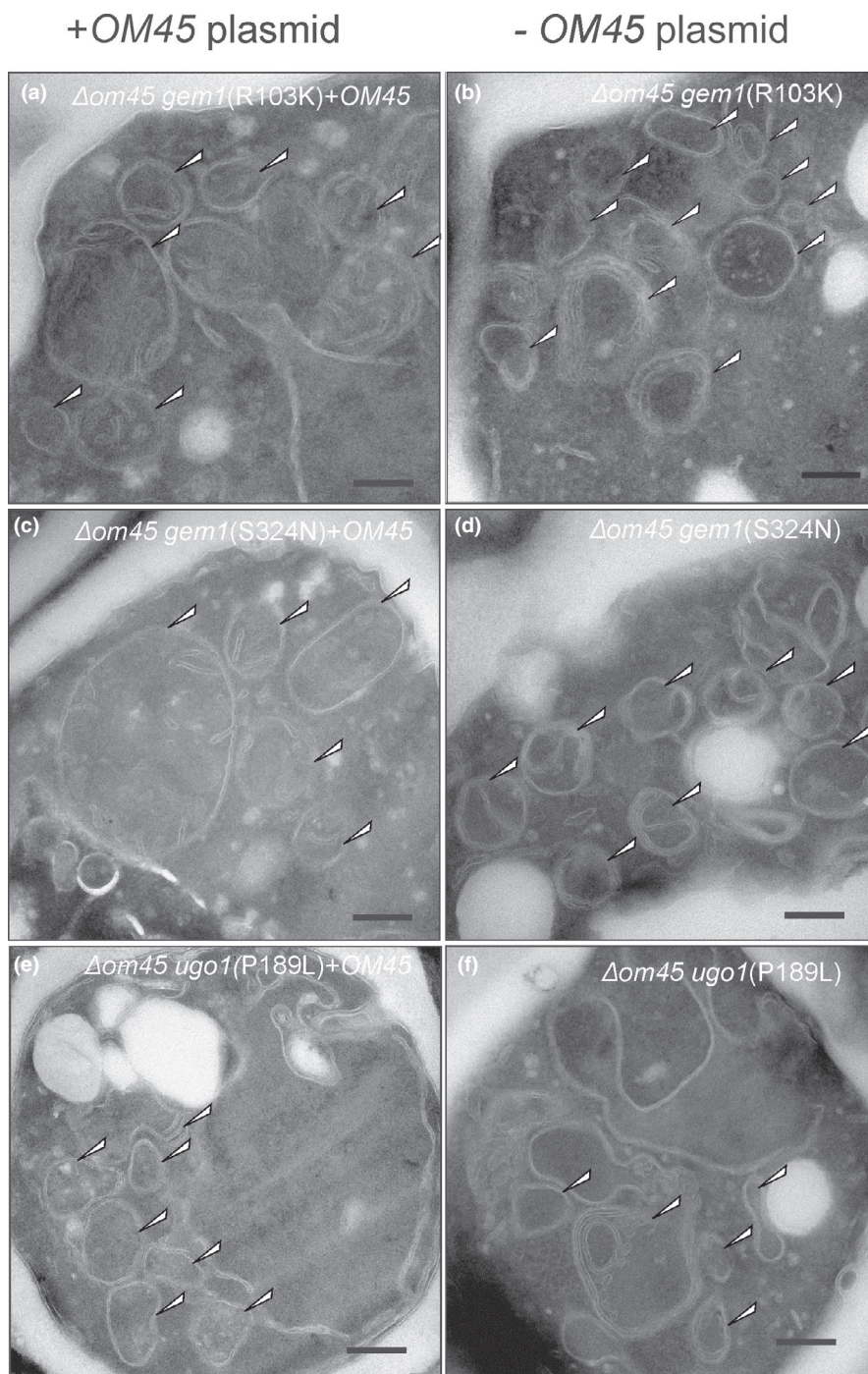(e) *Δom45 ugo1*(P189L)+*OM45*

(f) *Δom45 ugo1*(P189L)

FIGURE 4 Inner mitochondrial membrane folding is distorted in synthetic petite mutants upon loss of the OM45 plasmid. Electron micrographs of the synthetic petite mutants (a, c, e) with pTSV30OM45 and (b, d, f) without pTSV30OM45. The gem1 synthetic petites (b and d) show an improvement of cristae structure in the presence of the OM45 carrying plasmid (a and c). The ugo1 mutant, which has a highly disturbed mitochondrial membrane structure (f), also shows mitochondria with a more regular shape in the presence of OM45 (e). Arrows point at mitochondria. Cells were grown o/n in liquid synthetic complete media supplemented with glucose (2%). Arrows indicate mitochondria. Scale bar 200 nm

petite mutant was strongly reduced. The pTSV30*OM45* construct as well as the plasmid harboring an intact copy of *UGO1* rescued the respiratory growth of the reconstructed mutant (Figure A4).

The reconstruction of the mutants confirmed the negative synthetic interaction of the *om45* deletion with the *ugo1* and *gem1* mutations. As Ugo1p is poorly defined and the synthetic petite interaction was more robust for the reconstructed Δ*om45*Δ*gem1* mutant strains, we decided to focus on the *gem1/om45* interaction for our further analyses.

As analysis of the initial SPMs indicated severe mitochondrial ultrastructure morphology changes, we investigated the Δ*gem1*Δ*om45* double deletion mutant using electron microscopy. Because our previous analyses of the SPMs suggested increased mtDNA loss of the mutants upon non-selective growth on fermentable carbon sources, all cells used for the ultrastructure analysis were maintained and grow on media containing glycerol as the sole carbon source. The Δ*gem1*Δ*om45* double mutant cells are viable but extremely slow growers on this media (see also below for mtDNA content). Electron microscopy analysis of the Δ*om45*Δ*gem1* double mutant revealed mitochondrial membrane defects (Figure 5b) similar to the phenotype we observed in the SPMs (Figure 4b,d). The cristae structure of the IMM was severely
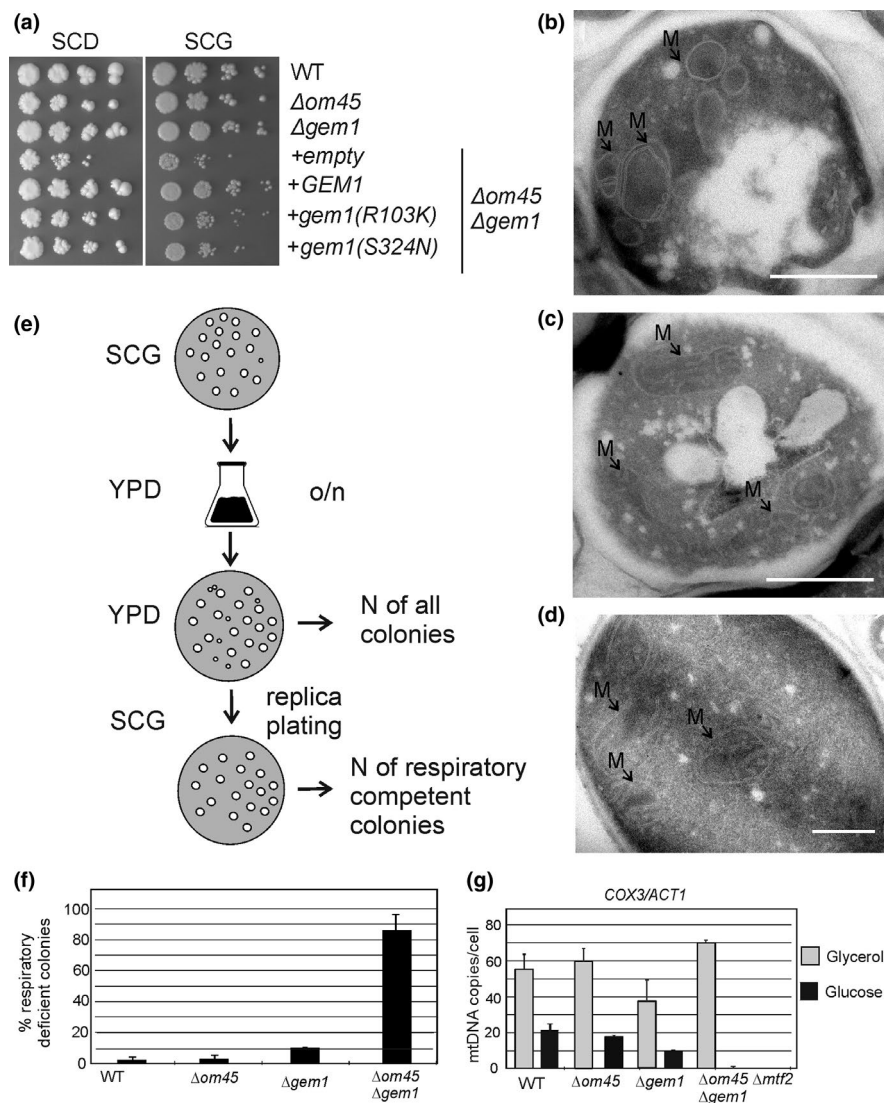
FIGURE 5 Growth phenotypes of reconstructed SPMs, mitochondrial morphology changes, and mtDNA loss of the W1536 8B Δom45Δgem1 strain. (a) The Δom45Δgem1 strain exhibits a synthetic petite phenotype, already apparent from the slow growth on SCD media. The SPM-derived gem1 mutant alleles only partially rescue growth in comparison to WT GEM1. Yeast strains were grown overnight in appropriate SC or SC selective liquid medium supplemented with glycerol. Cultures were normalized to OD595 = 1.0 and serial 10-fold dilutions were spotted onto SC solid media supplemented with glucose (2%) or glycerol (3%). Photographs were taken after 3 and 5 days of growth at 30°C for yeast growing in glucose and glycerol media, respectively. (b) Electron micrograph of W1536 8B Δom45Δgem1 with similarly disturbed cristae structure as the SPMs in Figure 4. (c) The same strain carrying the 2μ OM45 plasmid, with improved cristae structure. Cells were grown for 4 days in liquid synthetic complete media supplemented with glycerol (3%). EM Scale bar: 500 nm. (d) Electron micrograph of WT strain W1536 8B mitochondria. Scale bar indicates 500 nm. (e) Scheme for testing the rate of petite formation. After prolonged growth on fermentable media, the Δgem1 strain exhibits a mild increase of the respiratory deficient fraction of cells, while the Δom45Δgem1 double mutant massively accumulates respiratory deficient cells. Strains were initially grown on SCG media. They were then inoculated in liquid SC media supplemented with glucose (2%), grown overnight, and plated on solid rich YP media supplemented with glucose (2%). After 7 days of incubation at 30°C colonies were counted, and replicas plated on solid SC media supplemented with glycerol (3%). The number of the petite colonies = number of colonies on YPD plate minus number of colonies on SCG plate (N = 3). (f) A statistical representation of experiment described in (e). (g) ddPCR analysis of mtDNA content in cells grown on glucose or glycerol. All the yeast strains were transferred from an SCG plate on a YPD (2% glucose) plate (mother plate). Individual colonies from the mother plate were re-streaked on YPD plates several times and checked on the YPG plate for respiration competence. For genomic DNA isolation, all the strains were grown on YPD (2% glucose) liquid media overnight. Negative control: BY4741Δmtf2 (rho0 strain).

disturbed or completely absent. However, when these cells were transformed with a plasmid carrying *OM45*, cristae were restored (Figure 5c) and the mitochondria in the transformed strain were much closer to the appearance of WT organelles (Figure 5d), again mimicking the behavior of the SPM strains (Figure 4a,c). Overall, the reconstructed mutants, as well as the Δom45Δgem1 double deletion mutant, very closely resembled the original SPMs in their phenotypes.

3.5 | The Δom45Δgem1 strain generates petites at a high frequency when grown on fermentable media

While W1536 8B Δgem1Δom45 cells can be maintained indefinitely growing, albeit slowly, on glycerol media, a large fraction of the W1536 8B Δgem1Δom45 cells similarly to original SPM became completely respiratory deficient after just a brief growth phase on glucose media and could not be rescued anymore with plasmids carrying OM45 or the GEM1. Similarly, we observed that the original synthetic petite mutants, once they had lost the initial OM45 plasmid upon maintenance on glucose-containing medium, could not be rescued again by the retransformation with a 2μ OM45 plasmid.

We compared the frequency of generation of petites between W1536 8B Δom45, W1536 8B Δgem1, and W1536 8B Δom45Δgem1 strains, starting from cells growing on glycerol. After transfer to liquid YPD with a fermentable carbon source and overnight growth, cells were plated on a YPD plate, grown 4–5 days until proper colonies were formed, and subsequently replica plated onto non-fermentable SCG media (Figure 5e). W1536 8B Δom45 formed only very few respiratory deficient petite colonies. The W1536 8B Δgem1 mutant, which had previously been reported as losing mtDNA at a slightly elevated rate (Frederick et al., 2004), generated up to 15% of respiratory deficient colonies. The Δgem1Δom45 petite generation rate under the same conditions approached 85%. Therefore, the percentage of generation of respiratory deficient progeny was strongly increased in the Δom45Δgem1 double mutant compared to the individual deletion strains (Figure 5f).

We hypothesized that this high-frequency generation of petites is caused by mtDNA loss, which would be consistent with our inability to complement the SMPs with plasmids carrying wild-type copies of OM45 (or GEM1/UGO1) once the OM45 plasmid was lost.

3.6 | Synthetic petite mutants and mtDNA maintenance

Respiratory competence of the SPMs upon loss of the OM45 plasmid could not be restored upon retransformation. To investigate DNA copy number in wild type, Δom45, and Δgem1 mutants as well as the Δom45Δgem1 double mutant, we performed droplet digital PCR (ddPCR) probing for the mtDNA encoded COX3 (cytochrome c oxidase subunit 3) gene and nuclear-encoded ACT1 as reference. We found that the Δom45 mutant harbored mtDNA to wild-type levels, while the Δgem1 strain exhibited a slight reduction of mtDNA when grown on non-fermentable glycerol. Intriguingly, mtDNA content of the Δom45Δgem1 double deletion mutant was equivalent to, or perhaps even slightly increased when grown on glycerol (Figure 5g), as judged by the COX3 copy number signal. This is in stark contrast to the situation after the Δom45Δgem1 strain was subjected to overnight growth on fermentable YPD (Figure 5g) and mtDNA content was massively reduced (Figure 5g). The irreversible respiratory defect can be caused by either distortion of mitochondrial

genome integrity (rho⁻) or by its complete loss (rho⁰). A DAPI stain of SPM mutant cells showed a severe reduction of fluorescent spots co-localizing with mitochondrial matrix targeted GFP protein in absence of an OM45-carrying plasmid in the original Δom45gem1 SPMs (but not in the Δom45ugo1 SPM). We were able to confirm mtDNA phenotypes in the SPMs by droplet digital PCR quantitation using glucose-grown cells (Figure A5a and b). Interestingly, the gem1 SPMs maintain some mtDNA, unlike the Δom45Δgem1 mutant that completely loses mtDNA after growth on glucose. These results are more consistent with a reduction of mtDNA copy number in the SPMs, quickly leading to complete loss of mtDNA (rho⁰ cells) than with deletions within the mitochondrial DNA (rho⁻ mutations) as cause for secondary respiratory deficiency. They also clearly indicate that the morphology defect in the Δom45ugo1(P189L) SPM cannot be caused simply by mtDNA loss.

3.7 | Suppression of SPM phenotypes

In addition to UGO1, GEM1, and OM45, several other genes from the two rescuing library plasmids were identified and found to be suppressors of the mutations in gem1 and ugo1 genes (Table A1, Figures A6 and A7). Among these suppressors are genes encoding proteins of both the IMM (TIM44, SHY1, RTT109, and PET9) and the OMM (FZO1, MCP1, and PET54). The MCP1, PET54, and YPL109c partially rescued the growth of all three mutants, also from a single copy plasmid, but no mutation was detected in the genomic copies of the genes. Respiratory growth of Δom45 ugo1 (P189L) SPMs was restored by multicopy plasmids carrying TIM44, SHY1, DNM1, and FZO1.

3.8 | The functionality of Om45p fusion constructs

Om45p-GFP constructs have been used for mitochondrial morphology as well as autophagy studies due to Om45p abundance in the OMM during respiration and a previously reported lack of a phenotype for the W1536 8B Δom45 strain (Sesaki and Jensen, 2001; Kanki et al., 2009). The reconstructed synthetic petite mutant W1536 8B Δom45Δgem1 strain serves as a unique working tool for testing the functionality of Om45p and its fusion constructs.

First, we performed the complementation analysis of our mutants with an Om45p-GFP construct. The GFP-tagged OM45 single and multicopy plasmids (YCp33OM45-GFP and YEp195OM45-GFP) rescued the respiratory growth of the W1536 8B Δom45Δgem1 mutants much weaker than the plasmids carrying native OM45 (Figure 6a). This effect could be observed already in the sole W1536 8B Δom45 mutant, although much less pronounced (Figure 6b). Western blot analysis indicated that the levels of expression of Om45p and Om45-GFP were similar (Figure 6c).

In the case of the Δom45ugo1(P189L) SPM, the OM45-GFP is not rescuing the respiratory deficient phenotype of the mutant strain at all (Figure 6d).

3.9 | Phospholipid analysis

The results of the synthetic lethal screen implied that Gem1p and Om45p are likely to have some redundancy in their physiological roles. It has been suggested that Gem1p may regulate ER-mitochondria tethering, although the _gem1_ deletion alone is not sufficient to impair the phospholipid (PL) trafficking between ER and mitochondria (Nguyen et al., 2012). We decided to investigate whether _GEM1_ loss in combination with the _om45_ deletion leads to impaired ER-mitochondria interaction. Phosphatidylcholine (PC) synthesis from phosphatidylserine (PS) in yeast requires proper tethering of ER with OMM (Daum and Vance, 1997; Carman and Henry, 1999; Stone and Vance, 2000; Kornmann et al., 2011; Nguyen et al., 2012; Horvath and Daum, 2013). To develop an ER-mitochondria interaction assay we sought to take advantage of this dependence of the phospholipid biosynthesis process on a tight association of the two organelles.

In addition to the mitochondrial PS decarboxylation, there is a minor vacuolar/Golgi pathway in yeast involving Psd2p, which does not depend on mitochondria-ER interaction. To study exclusively the contribution of mitochondrial PS-synthesis, all strains were generated in a Δ_psd2_ background (Trotter et al., 1993; Trotter and Voelker, 1995; Voelker, 1997). If Om45p and Gem1p had a redundant function in mediating ER-mitochondria interaction, the Δ_psd2_Δ_gem1_Δ_om45_ triple knockout strain would be predicted to show an accumulation of PS and possibly depletion of phosphatidylethanolamine (PE) or PC due to impaired trafficking between ER and mitochondria. A suitable control is the isogenic W1536 8B Δ_psd1_Δ_psd2_ strain, where deletion of both PS decarboxylase enzymes severely compromises phospholipid metabolism, leading to accumulation of unprocessed PS. As additional controls, phospholipid profiles of W1536 8B Δ_gem1_ or W1536 8B Δ_om45_ deletion strains also lacking _psd2_ were

FIGURE 6 The complementation potency of Om45 is diminished by C-terminal GFP tagging. Spotting assay with the (a) W1536 8B Δom45Δgem1 and (b) W1536 8B Δom45 strain expressing Om45 or Om45-GFP from CEN (URA3) or 2µ (URA3) (multicopy) plasmids. Yeast strains carrying an indicated plasmid were grown overnight in a synthetic complete medium lacking uracil and supplemented with glycerol (3%). Cultures were normalized to OD595 = 1.0 and serial 10-fold dilutions were spotted onto synthetic complete solid media lacking uracil and supplemented with either glucose (2%) or glycerol (3%). Photographs were taken after 3 and 5 days of growth at 30°C for yeast growing in glucose and glycerol media, respectively. (c) Representative western blot image. Om45-GFP levels expressed in the Δom45 strain are comparable to Om45p levels expressed from the corresponding vector. Cells were grown at 30°C. Western blot probed with anti-OM45p rabbit serum and anti-rabbit antibodies conjugated to HRP. Imaging with BioRad ChemiDoc™. (d) SPM complementation with CEN and 2µ OM45 plasmids. Cells carrying a 2µ OM45(TRP1) plasmid and either of the test plasmids were plated on SCG-URA low TRP medium supplemented with 5′FAA for TRP1 plasmid counterselection. OM45-GFP (CEN) (low copy plasmid); OM45-GFP (2µ) (high copy plasmid); YCp33OM45 (+); YCplac33 (−) (empty plasmid)
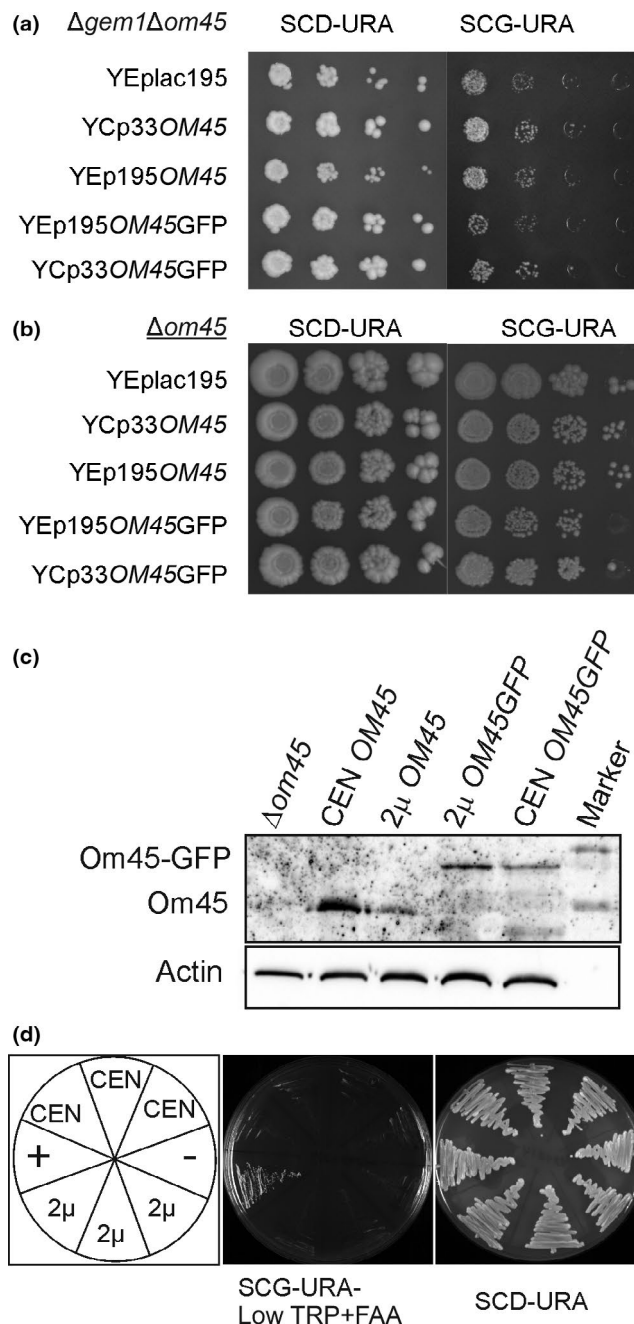
investigated to assess the effect of the individual deletions of these OMM proteins on phospholipid turnover.

UPLC-Q-Tof-MS was used to analyze the lipidomes of whole cells and of highly purified mitochondria from five different deletion strains grown on glycerol-containing media: W1536 8B Δ_om45_Δ_psd2_; W1536 8B Δ_gem1_Δ_psd2_; W1536 8B Δ_gem1_Δ_om45_Δ_psd2_; W1536 8B Δ_psd2_ and Δ_psd1_Δ_psd2_ (Figure A6). The W1536 8B Δ_psd1_Δ_psd2_ control strain lacking both PS decarboxylases is an auxotroph for ethanolamine required to produce the essential PE and PC phospholipids via the Kennedy pathway (McMaster, 2018). Hence, the growth media of all strains were supplemented with 2 mM ethanolamine. The growth of strains on glycerol is cumbersome especially for the very slow-growing Δ_gem1_Δ_om45_Δ_psd2_ variant, but as we

wanted to avoid lesions secondary to the original mutations, it was necessary to produce cell material under conditions that prevented mtDNA loss.

Our mass spectrometric PL analysis was consistent with the results of Vance et al., who demonstrated that PC is the most abundant PL in eukaryotic cells. PE and PI are also present in ample amounts, while PS, a precursor for PE and PC is quantitatively a minor phospholipid (Vance and Steenbergen, 2005) (Figure A8) The data are presented in the % ratios, with the total sample phospholipids set as 100% as well as PS/PE ratio.

As expected, the PS/PE ratio showed a clear increase in the W1536 8B Δpsd1Δpsd2 strain, where deletion of both PS decarboxylase enzymes severely compromised phospholipid metabolism and caused PS accumulation. W1536 8B Δgem1Δom45Δpsd2 did not show any increase in PS, and the PS/PE ratio in this strain was similar to the control W1536 8B Δom45Δpsd2, W1536 8B Δgem1Δpsd2 and W1536 8B Δpsd2 strains both in whole cell lipids extracts and in the highly pure mitochondria. Thus, neither the om45 deletion alone nor in combination with the gem1 deletion appear to affect the PS to PE conversion in yeast cells.

4 | DISCUSSION

The cellular role of Om45, one of the major proteins of the yeast OMM, has remained obscure for several decades. The protein is fixed to the OMM via an N-terminal α-helical membrane anchor, and for a long time, it was believed that the major solvent-exposed C-terminal domain of Om45 was facing the cytosol. Hence the place of action of Om45 was suspected to be on the mitochondrial outer surface. In 2012, Lauffer et al. first reported evidence for the IMS orientation of Om45p (Lauffer et al., 2012). Data obtained by us in this present study are consistent with the configuration proposed in the latter work.

The discovery of yeast Miro GTPase in the early 2000s initially caused a stir in the mitochondrial community (Frederick et al., 2004). Reports of a role of Gem1 as a partner of the ERMES complex, regulating mitochondria-ER interactions and phospholipid exchange (Kornmann et al., 2011) could not be unequivocally confirmed (Nguyen et al., 2012). Here, we present evidence for a collaborative role of Om45p and Gem1p in mitochondrial inner membrane organization. We were unable to find any support for a function of these proteins, either alone or in combination, in phospholipid trafficking. Our results imply that the action of Gem1p and Om45p is oriented toward the IMM and required for cristae and mtDNA maintenance.

Our synthetic lethal screen based on the colony color-sectoring assay revealed two evolutionarily conserved genes, GEM1 and UGO1, as interacting genetically with OM45. The SPMs obtained in our screen as well as the mutant reconstruction variants showed impaired IMM organization in the absence of Om45 where they also become respiratory deficient due to progressive mtDNA loss. The data speak in favor of at least partial redundancy of Om45p with Gem1p and Ugo1p in terms of their physiological function. Unlike

Gem1 and Ugo1, which are conserved in higher eukaryotes, no homolog of Om45 could be identified in mammals. Deletions of either GEM1 or UGO1 have been shown to affect mitochondria morphology and mtDNA maintenance in yeast. While Δgem1 strains experience only a mild increase of mtDNA loss (Frederick et al., 2004), the ugo1 deletion results in a rho^0 phenotype (Sesaki and Jensen, 2001). Our Δom45, Δgem1 double deletion strain, and gem1 SPMs display a similar loss of mtDNA.

The Ugo1 protein has been reported to bring together OMM and IMM by acting as a scaffold between Mgm1p and Fzo1p proteins in the IMM and the OMM, respectively (Sesaki and Jensen, 2004; Coonrod et al., 2007; Anton et al., 2011). There have been speculations about a possible lipid mixing role of Ugo1 required for mitochondrial fusion (Hoppins et al., 2009). Cells lacking Ugo1p fail to form a tubular mitochondrial network, shifting the mitochondrial dynamics balance toward fragmentation, which ultimately leads to complete loss of mtDNA (Sesaki and Jensen, 2001; Sesaki and Jensen, 2004; Itoh et al., 2013). Mutations in the Ugo1p-like protein SLC25A46 in humans were reported to cause an optic atrophy spectrum disorder. In contrast to the phenotype of UGO1 deletions in yeast, the knockdown of SLC25A46 was found to cause mitochondrial hyperfusion, while overexpression of the mammalian UGO1 homolog led to mitochondrial fragmentation (Abrams et al., 2015). While we did not pursue any deeper analysis of the Δom45, ugo1 SPM, our ability to identify such an interaction in general supports our conclusions on the functions of Om45p and Gem1p.

Gem1p is the yeast homolog of human Miro GTPase (Frederick et al., 2004; Tang, 2015). In the absence of Gem1p, yeast mitochondria exhibit a pronounced defect in mitochondrial cellular distribution and morphology, forming collapsed tubular and globular mitochondria with an irregular diameter (Frederick et al., 2004). Unlike its mammalian homolog, the role of Gem1p in interaction with the cytoskeleton has not been observed in yeast. Instead, deletion of GEM1 has been reported to affect the size and the number of mitochondria-ER encounter structures (ERMES) in S. cerevisiae. The role of Gem1p in ERMES function has been controversial (Nguyen et al., 2012). In our eyes, the synthetic defect in Δom45/gem1(R103K), Δom45/gem1(S324N), and Δom45 /ugo1(P189L) can be only explained by (partially) redundant function(s) of the proteins acting in parallel. Inspired by experiments described previously for Δgem1 strains by the Shaw group (Nguyen et al., 2012), we examined the phospholipid composition of the Δom45 and Δgem1 strains to determine if the redundant functions of Om45p and Gem1p may be obscuring an effect of the Δgem1 mutation on phospholipid levels and, by extension, on ERMES function. Like in the Nguyen et al. report, PS conversion to PE and further to PC in the yeast carrying single deletions of Δom45, or Δgem1 as well as in the Δom45Δgem1 double deletion was not distinguishable from the control. Hence, we found no evidence for a possible common role of the two proteins in mediating the tethering of mitochondria to the ER.

Genetic interaction of OM45 with GEM1 was previously reported in a high throughput study describing components of the mitochondrial contact site (MICOS) complex (Hoppins et al., 2011), a

scaffold-like structure required for mitochondrial IMM organization (Alkhaja et al., 2012; Harner et al., 2011; van der Laan et al., 2012; Pfanner et al., 2014; Rabl et al., 2009; Zerbes et al., 2012). Our SPMs are characterized by strong distortion of IMM folding, which may be a reason for progressive mtDNA loss. We argue for the IMM folding disturbance as the cause of the mtDNA loss in the SPMs rather than a result thereof based on three observations: First, mitochondrial morphology in the mutants is not consistent with the morphology observed in rho^0 cells (compare Figure 2/Figure A5 and (Sesaki & Jensen, 2001, Figure 3)), and mitochondrial ultrastructural changes in rho0 cells differ from the changes observed in the SPMs (Figure 4, Figure A2). Second, and even more compelling, we can show that the IMM disturbance is observable already in cells that still harbor mtDNA (Figure 5b, representative micrograph of a Δom45Δgem1 cell grown on glycerol, Figure 5g, mtDNA content of Δom45Δgem1 cells grown on glycerol). Lastly, at least the ugo1(P189L) SPM clearly maintains mtDNA despite severe mitochondrial morphology and ultrastructural defects (Figure A5).

Intriguingly, the combination of mutations in OMM proteins causes the strongest phenotype in the IMM folding. The reported IMS orientation of Om45p (Lauffer et al., 2012; Song et al., 2014; Wenz et al., 2014), however, makes a role of the protein in the mediation of OMM and IMM contacts plausible.

In addition to the *GEM1* and *UGO1* isolates obtained by library complementation, we found several multicopy suppressors that can rescue the synthetic petite phenotypes. Among them are *FZO1*, *MCP1* encoding OMM proteins, as well as *TIM44*, *SHY1*, *PET9*, and *PET54* encoding IMM proteins. The function of Mcp1p is not well understood, but it appears to be involved in lipid homeostasis (Tan et al., 2013). Physical interaction of Fzo1 with Ugo1 is required for mitochondrial fusion (Sesaki and Jensen, 2004; Coonrod et al., 2007; Anton et al., 2011). Shy1 and Pet54 play roles in respiratory complex IV component expression and assembly. Shy1p is necessary for full expression of mitochondrial *COX1* in the yeast model of Leigh's syndrome (Barrientos et al., 2002). The PET54 gene of Saccharomyces cerevisiae: characterization of a nuclear gene encoding a mitochondrial translational activator and subcellular localization of its product (Costanzo et al., 1989). Pet9 (Aac2) is an ADP/ATP carrier of the IMM, affecting the level of ATP in the IMS and also found to be associated with MICOS and Om45-Om14-Por1 protein complexes (Lauffer et al., 2012; Linden et al., 2020). Tim44 is an essential component of the TIM23 complex (Blom et al., 1993; Pfanner et al., 1996; Popov-Čeleketić et al., 2008), physically interacting with Ssc1 (D'Silva et al., 2004; Liu et al., 2001; Wadhwa et al., 2002). While we do not clearly understand the mechanisms of multicopy suppression by these factors as a whole they may point toward membrane fusion and protein import into the mitochondrial matrix as well as respiratory chain assembly functions.

Although Om45p and Gem1p (as well as Ugo1p) reside on the OMM, our results firmly indicate the IMM is most strongly affected by their loss of function. Our investigation of the role of Om45 under growth conditions that have not been tested before as well as the genetic and physical interactions of Om45p that were identified during this work revealed several cellular processes affected by Om45p. In particular, mitochondrial morphology maintenance, IMM folding, and mtDNA inheritance are affected by the absence of Om45p in a *gem1* (or *ugo1*) mutant strain background. Taken together, the mutant morphology, growth phenotypes, multicopy suppressors, and phospholipidome studies we present here point to a possible role of Om45 and Gem1 in IMM homeostasis and mediation of interaction between the two mitochondrial membranes. We find no direct evidence for the role of these proteins in ER/mitochondrial phospholipid exchange processes.

An additional aspect of our work is that the phenotype of the synthetic mutant strains is strongly dependent on the presence of Om45p, which makes these synthetic petites a unique system for testing the functionality of Om45p constructs. Our results indicate that the C-terminal tagging of Om45p interferes with its functions. GFP-tagged Om45p did not complement the synthetic mutants and displayed a growth defect in the Δgem1Δom45 and Δom45 strain backgrounds. In light of our observation of the role of Om45p in mitochondrial morphology maintenance, such constructs may not be the best choice as a marker for mitochondrial morphology studies for which it has been used previously (Sesaki and Jensen, 2001; Sesaki et al., 2003).

ETHICS STATEMENT

None required.

CONFLICT OF INTEREST

None declared.

AUTHOR CONTRIBUTIONS

Antonina Shvetsova: Conceptualization (equal); Formal analysis (lead); Investigation (lead); Methodology (equal); Project administration (equal); Validation (lead); Visualization (lead); Writing-original draft (lead); Writing-review & editing (lead). **Ali Julfiker Masud:** Conceptualization (supporting); Formal analysis (supporting); Investigation (supporting); Methodology (supporting); Project administration (supporting); Writing-review & editing (supporting). **Laura Schneider:** Investigation (supporting); Methodology (supporting); Writing-original draft (supporting); Writing-review & editing (supporting). **Geoffray Monteuuis:** Investigation (supporting); Methodology (supporting); Writing-original draft (supporting); Writing-review & editing (supporting). **Ulrich Bergmann:** Conceptualization (supporting); Formal analysis (equal); Investigation (supporting); Methodology (equal); Project administration (supporting); Supervision (equal);

Validation (lead); Writing-original draft (supporting); Writing-review & editing (supporting). **Ilkka Miinalainen:** Formal analysis (equal); Investigation (supporting); Methodology (equal); Writing-original draft (supporting); Writing-review & editing (supporting). **J. Kalervo Hiltunen:** Conceptualization (supporting); Formal analysis (supporting); Methodology (supporting); Project administration (supporting); Supervision (equal); Writing-original draft (supporting); Writing-review & editing (supporting). **Alexander Kastaniotis:** Conceptualization (lead); Data curation (lead); Formal analysis (lead); Funding acquisition (equal); Investigation (equal); Methodology (lead); Project administration (lead); Resources (equal); Software (equal); Supervision (lead); Validation (equal); Visualization (equal); Writing-original draft (equal); Writing-review & editing (equal).

DATA AVAILABILITY STATEMENT

All data are provided in full in this paper. Data used to generate the mitochondrial morphology graph in Figure 3, the digital droplet PCR mtDNA graph inf Figure 5, and the phospholipidome analysis graphs of Figure A8 have been deposited in Fairdata IDA: https://doi.org/10.23729/30104e54-a79c-477d-9c76-d6722b0d4d53

ORCID

Ali J. Masud https://orcid.org/0000-0002-4126-6513
Ulrich Bergmann https://orcid.org/0000-0002-8684-9640
Geoffray Monteuuis https://orcid.org/0000-0001-7193-7771
J. Kalervo Hiltunen https://orcid.org/0000-0002-3073-9602
Alexander J. Kastaniotis https://orcid.org/0000-0003-3624-9214

REFERENCES

Abrams, A. J., Hufnagel, R. B., Rebelo, A., Zanna, C., Patel, N., Gonzalez, M. A., Campeanu, I. J., Griffin, L. B., Groenewald, S., Strickland, A. V., Tao, F., Speziani, F., Abreu, L., Schüle, R., Caporali, L., La Morgia, C., Maresca, A., Liguori, R., Lodi, R., ... Dallman, J. E. (2015). Mutations in SLC25A46, encoding a UGO1-like protein, cause an optic atrophy spectrum disorder. *Nature Genetics*, *47*(8), 926–932. https://doi.org/10.1038/ng.3354

Alkhaja, A. K., Jans, D. C., Nikolov, M., Vukotic, M., Lytovchenko, O., Ludewig, F., Schliebs, W., Riedel, D., Urlaub, H., Jakobs, S., & Deckers, M. (2012). MINOS1 is a conserved component of mitofilin complexes and required for mitochondrial function and cristae organization. *Molecular Biology of the Cell*, *23*, 247–257. https://doi.org/10.1091/mbc.e11-09-0774

Amberg, D. C., Burke, D. J., & Strathern, J. N. (2005). *Methods in yeast genetics: A cold spring harbor laboratory course manual, 2005 edition*. Cold Spring Harbor Laboratory Press.

Anton, F., Fres, J. M., Schauss, A., Pinson, B., Praefcke, G. J. K., Langer, T., & Escobar-Henriques, M. (2011). Ugo1 and Mdm30 act sequentially during Fzo1-mediated mitochondrial outer membrane fusion. *Journal of Cell Science*, *124*, 1126–1135. https://doi.org/10.1242/jcs.073080

Ausubel, F. M., Brent, R. E., Kingston, D. D., Moore, J. G., & Seidman, J. A. (Eds), *Current protocols in molecular biology*. New York, NY: John Wiley and Sons.

Barrientos, A., Knorr, D., & Tzagoloff, A. (2002). Shy1p is necessary for full expression of mitochondrial COX1 in the yeast model of Leigh's syndrome. *EMBO Journal*, *21*, 43–52. https://doi.org/10.1093/emboj/21.1.43

Blom, J., Kübrich, M., Rassow, J., Voos, W., Dekker, P. J., Maarse, A. C., Meijer, M., & Pfanner, N. (1993). The essential yeast protein MIM44 (encoded by MPI1) is involved in an early step of preprotein translocation across the mitochondrial inner membrane. *Molecular and Cellular Biology*, *13*, 7364–7371. https://doi.org/10.1128/MCB.13.12.7364

Bonneaud, N., Ozier-Kalogeropoulos, O., Li, G., Labouesse, M., Minvielle-Sebastia, L., & Lacroute, F. (1991). A family of low and high copy replicative, integrative and single-stranded *S. cerevisiae/E. coli* shuttle vectors. *Yeast*, *7*, 609–615. https://doi.org/10.1002/yea.320070609

Burri, L., Vascotto, K., Gentle, I. E., Chan, N. C., Beilharz, T., Stapleton, D. I., Ramage, L., & Lithgow, T. (2006). Integral membrane proteins in the mitochondrial outer membrane of *Saccharomyces cerevisiae*. *FEBS Journal*, *273*, 1507–1515. https://doi.org/10.1111/j.1742-4658.2006.05171.x

Carman, G. M., & Henry, S. A. (1999). Phospholipid biosynthesis in the yeast *Saccharomyces cerevisiae* and interrelationship with other metabolic processes. *Progress in Lipid Research*, *38*, 361–399.

Chen, D., Yang, B., & Kuo, T. (1992). One-step transformation of yeast in stationary phase. *Current Genetics*, *21*, 83–84. https://doi.org/10.1007/BF00318659

Christie, W. W. (2003). *Lipid analysis. isolation, separation, identification and structural analysis of lipids*. The Oily Press Ltd.

Coonrod, E. M., Karren, M. A., & Shaw, J. M. (2007). Ugo1p is a multipass transmembrane protein with a single carrier domain required for mitochondrial fusion. *Traffic*, *8*, 500–511. https://doi.org/10.1111/j.1600-0854.2007.00550.x

Costanzo, M. C., Seaver, E. C., & Fox, T. D. (1989). The *PET54* gene of *Saccharomyces cerevisiae*: characterization of a nuclear gene encoding a mitochondrial translational activator and subcellular localization of its product. *Genetics*, *122*(2), 297–305. https://doi.org/10.1093/genetics/122.2.297

Daum, G., & Vance, J. E. (1997). Import of lipids into mitochondria. *Progress in Lipid Research*, *36*, 103–130. https://doi.org/10.1016/S0163-7827(97)00006-4

D'Silva, P., Liu, Q., Walter, W., & Craig, E. A. (2004). Regulated interactions of mtHsp70 with Tim44 at the translocon in the mitochondrial inner membrane. *Nature Structural & Molecular Biology*, *11*, 1084–1091. https://doi.org/10.1038/nsmb846

Frederick, R. L., McCaffery, J. M., Cunningham, K. W., Okamoto, K., & Shaw, J. M. (2004). Yeast Miro GTPase, Gem1p, regulates mitochondrial morphology via a novel pathway. *Journal of Cell Biology*, *167*, 87–98. https://doi.org/10.1083/jcb.200405100

Gietz, R. D., & Sugino, A. (1988). New yeast *Escherichia coli* shuttle vectors constructed with in vitro mutagenized yeast genes lacking six-base pair restriction sites. *Gene*, *74*, 527–534.

Gietz, R. D., & Woods, R. A. (2002). Transformation of yeast by lithium acetate/single-stranded carrier DNA/polyethylene glycol method. *Meth Enzymol*, *350*, 87–96.

Goldstein, A. L., & McCusker, J. H. (1999). Three new dominant drug resistance cassettes for gene disruption in *Saccharomyces cerevisiae*. *Yeast*, *15*, 1541–1553. https://doi.org/10.1002/(SICI)1097-0061(199910)15:14<1541:AID-YEA476>3.0.CO;2-K

Griffith, J., Mari, M., De Mazière, A., & Reggiori, F. (2008). A cryosectioning procedure for the ultrastructural analysis and the immunogold labelling of yeast *Saccharomyces cerevisiae*. *Traffic*, *9*, 1060–1072. https://doi.org/10.1111/j.1600-0854.2008.00753.x

Harington, A., Herbert, C., Tung, B., Getz, G., & Slonimski, P. (1993). Identification of a new nuclear gene (CEM1) encoding a protein homologous to a β-ketoacyl synthase which is essential for mitochondrial respiration in Saccharomyces cerevisiae. *Molecular Microbiology*, *9*, 545–555.

Harner, M., Körner, C., Walther, D., Mokranjac, D., Kaesmacher, J., Welsch, U., Griffith, J., Mann, M., Reggiori, F., & Neupert, W. (2011).

The mitochondrial contact site complex, a determinant of mitochondrial architecture. *EMBO Journal*, 30, 4356–4370. https://doi.org/10.1038/emboj.2011.379

Hoffman, C. S., & Winston, F. (1987). A ten-minute DNA preparation from yeast efficiently releases autonomous plasmids for transformaion of *Escherichia coli*. *Gene*, 57, 267–272. https://doi.org/10.1016/0378-1119(87)90131-4

Hoppins, S., Collins, S. R., Cassidy-Stone, A., Hummel, E., DeVay, R. M., Lackner, L. L., Westermann, B., Schuldiner, M., Weissman, J. S., & Nunnari, J. (2011). A mitochondrial-focused genetic interaction map reveals a scaffold-like complex required for inner membrane organization in mitochondria. *Journal of Cell Biology*, 195, 323–340. https://doi.org/10.1083/jcb.201107053

Hoppins, S., Horner, J., Song, C., McCaffery, J. M., & Nunnari, J. (2009). Mitochondrial outer and inner membrane fusion requires a modified carrier protein. *Journal of Cell Biology*, 184, 569–581. https://doi.org/10.1083/jcb.200809099

Horvath, S. E., & Daum, G. (2013). Lipids of mitochondria. *Progress in Lipid Research*, 52, 590–614. https://doi.org/10.1016/j.plipres.2013.07.002

Itoh, K., Tamura, Y., Iijima, M., & Sesaki, H. (2013). Effects of Fcj1-Mos1 and mitochondrial division on aggregation of mitochondrial DNA nucleoids and organelle morphology. *Molecular Biology of the Cell*, 24, 1842–1851. https://doi.org/10.1091/mbc.e13-03-0125

Jones, B. A., & Fangman, W. L. (1992). Mitochondrial DNA maintenance in yeast requires a protein containing a region related to the GTP-binding domain of dynamin. *Genes & Development*, 6, 380–389. https://doi.org/10.1101/gad.6.3.380

Kanki, T., Kang, D., & Klionsky, D. J. (2009). Monitoring mitophagy in yeast. *Autophagy*, 5, 1186–1189.

Kastaniotis, A. J., Autio, K. J., Sormunen, R. T., & Hiltunen, J. K. (2004). Htd2p/Yhr067p is a yeast 3-hydroxyacyl-ACP dehydratase essential for mitochondrial function and morphology. *Molecular Microbiology*, 53, 1407–1421. https://doi.org/10.1111/j.1365-2958.2004.04191.x

Knop, M., Siegers, K., Pereira, G., Zachariae, W., Winsor, B., Nasmyth, K., & Schiebel, E. (1999). Epitope tagging of yeast genes using a PCR-based strategy: more tags and improved practical routines. *Yeast*, 15, 963–972. https://doi.org/10.1002/(SICI)1097-0061(199907)15:10B<963:AID-YEA399>3.0.CO;2-W

Kornmann, B., Osman, C., & Walter, P. (2011). The conserved GTPase Gem1 regulates endoplasmic reticulum-mitochondria connections. *Proceedings of the National Academy of Sciences, USA*, 108, 14151–14156. https://doi.org/10.1073/pnas.1111314108

Kursu, V. A., Pietikäinen, L. P., Fontanesi, F., Aaltonen, M. J., Suomi, F., Raghavan Nair, R., Schonauer, M. S., Dieckmann, C. L., Barrientos, A., Hiltunen, J. K., & Kastaniotis, A. J. (2013). Defects in mitochondrial fatty acid synthesis result in failure of multiple aspects of mitochondrial biogenesis in Saccharomyces cerevisiae. *Molecular Microbiology*, 90, 824–840.

Laemmli, U. K. (1970). Cleavage of structural proteins during the assembly of the head of bacteriophage T4. *Nature*, 227, 680–685. https://doi.org/10.1038/227680a0

Lauffer, S., Mabert, K., Czupalla, C., Pursche, T., Hoflack, B., Rodel, G., & Krause-Buchholz, U. (2012). *Saccharomyces cerevisiae* porin pore forms complexes with mitochondrial outer membrane proteins Om14p and Om45p. *Journal of Biological Chemistry*, 287, 17447–17458. https://doi.org/10.1074/jbc.M111.328328

Lee, M. S., Henry, M., & Silver, P. A. (1996). A protein that shuttles between the nucleus and the cytoplasm is an important mediator of RNA export. *Genes & Development*, 10, 1233–1246. https://doi.org/10.1101/gad.10.10.1233

Linden, A., Deckers, M., Parfentev, I., Pflanz, R., Homberg, B., Neumann, P., Ficner, R., Rehling, P., & Urlaub, H. (2020). A cross-linking mass spectrometry approach defines protein interactions in yeast

mitochondria. *Molecular & Cellular Proteomics*, 19, 1161–1178. https://doi.org/10.1074/mcp.RA120.002028

Liu, Q., Krzewska, J., Liberek, K., & Craig, E. A. (2001). Mitochondrial Hsp70 Ssc1: role in protein folding. *Journal of Biological Chemistry*, 276, 6112–6118. https://doi.org/10.1074/jbc.M009519200

Mannella, C. A. (1992). The 'ins' and 'outs' of mitochondrial membrane channels. *Trends in Biochemical Sciences*, 17, 315–320. https://doi.org/10.1016/0968-0004(92)90444-E

McMaster, C. R. (2018). From yeast to humans–roles of the Kennedy pathway for phosphatidylcholine synthesis. *FEBS Letters*, 592, 1256–1272. https://doi.org/10.1002/1873-3468.12919

Nguyen, T. T., Lewandowska, A., Choi, J. Y., Markgraf, D. F., Junker, M., Bilgin, M., Ejsing, C. S., Voelker, D. R., Rapoport, T. A., & Shaw, J. M. (2012). Gem1 and ERMES do not directly affect phosphatidylserine transport from ER to mitochondria or mitochondrial inheritance. *Traffic*, 13, 880–890.

Ohlmeier, S., Kastaniotis, A. J., Hiltunen, J. K., & Bergmann, U. (2004). The yeast mitochondrial proteome, a study of fermentative and respiratory growth. *Journal of Biological Chemistry*, 279, 3956–3979. https://doi.org/10.1074/jbc.M310160200

Pfanner, N., Douglas, M. G., Endo, T., Hoogenraad, N. J., Jensen, R. E., Meijer, M., Neupert, W., Schatz, G., Schmitz, U. K., & Shore, G. C. (1996). Uniform nomenclature for the protein transport machinery of the mitochondrial membranes. *Trends in Biochemical Sciences*, 21, 51–52. https://doi.org/10.1016/S0968-0004(96)80179-4

Pfanner, N., van der Laan, M., Amati, P., Capaldi, R. A., Caudy, A. A., Chacinska, A., Darshi, M., Deckers, M., Hoppins, S., Icho, T., Jakobs, S., Ji, J., Kozjak-Pavlovic, V., Meisinger, C., Odgren, P. R., Park, S. K., Rehling, P., Reichert, A. S., Sheikh, M. S., ... Nunnari, J. (2014). Uniform nomenclature for the mitochondrial contact site and cristae organizing system. *Journal of Cell Biology*, 204, 1083–1086. https://doi.org/10.1083/jcb.201401006

Platta, H., Girzalsky, W., & Erdmann, R. (2004). Ubiquitination of the peroxisomal import receptor Pex5p. *Biochemical Journal*, 384, 37–45. https://doi.org/10.1042/BJ20040572

Popov-Čeleketić, D., Mapa, K., Neupert, W., & Mokranjac, D. (2008). Active remodelling of the TIM23 complex during translocation of preproteins into mitochondria. *EMBO Journal*, 27, 1469–1480. https://doi.org/10.1038/emboj.2008.79

Rabl, R., Soubannier, V., Scholz, R., Vogel, F., Mendl, N., Vasiljev-Neumeyer, A., Körner, C., Jagasia, R., Keil, T., Baumeister, W., Cyrklaff, M., Neupert, W., & Reichert, A. S. (2009). Formation of cristae and crista junctions in mitochondria depends on antagonism between Fcj1 and Su e/g. *Journal of Cell Biology*, 185, 1047–1063. https://doi.org/10.1083/jcb.200811099

Riezman, H., Hay, R., Gasser, S., Daum, G., Schneider, G., Witte, C., & Schatz, G. (1983). The outer membrane of yeast mitochondria: isolation of outside-out sealed vesicles. *EMBO Journal*, 2, 1105–1111. https://doi.org/10.1002/j.1460-2075.1983.tb01553.x

Sesaki, H., & Jensen, R. E. (2001). UGO1 encodes an outer membrane protein required for mitochondrial fusion. *Journal of Cell Biology*, 152, 1123–1134. https://doi.org/10.1083/jcb.152.6.1123

Sesaki, H., & Jensen, R. E. (2004). Ugo1p links the Fzo1p and Mgm1p GTPases for mitochondrial fusion. *Journal of Biological Chemistry*, 279, 28298–28303. https://doi.org/10.1074/jbc.M401363200

Sesaki, H., Southard, S. M., Yaffe, M. P., & Jensen, R. E. (2003). Mgm1p, a dynamin-related GTPase, is essential for fusion of the mitochondrial outer membrane. *Molecular Biology of the Cell*, 14, 2342–2356. https://doi.org/10.1091/mbc.e02-12-0788

Song, J., Tamura, Y., Yoshihisa, T., & Endo, T. (2014). A novel import route for an N-anchor mitochondrial outer membrane protein aided by the TIM23 complex. *EMBO Reports*. https://doi.org/10.1002/embr.201338142

Stone, S. J., & Vance, J. E. (2000). Phosphatidylserine synthase-1 and -2 are localized to mitochondria-associated membranes. *Journal of*

Biological Chemistry, _275_, 34534–34540. https://doi.org/10.1074/jbc.M002865200

Studier, F. W., & Moffatt, B. A. (1986). Use of bacteriophage T7 RNA polymerase to direct selective high-level expression of cloned genes. _Journal of Molecular Biology_, _189_, 113–130. https://doi.org/10.1016/0022-2836(86)90385-2

Studier, F. W., Rosenberg, A. H., Dunn, J. J., & Dubendorff, J. W. (1990). Use of T7 RNA polymerase to direct expression of cloned genes. _Meth Enzymol_, _185_, 60–89.

Tan, T., Ozbalci, C., Brugger, B., Rapaport, D., & Dimmer, K. S. (2013). Mcp1 and Mcp2, two novel proteins involved in mitochondrial lipid homeostasis. _Journal of Cell Science_, _126_, 3563–3574. https://doi.org/10.1242/jcs.121244

Tang, B. L. (2015). MIRO GTPases in mitochondrial transport. _Homeostasis and Pathology_, _5_, 1. https://doi.org/10.3390/cells5010001

Trotter, P. J., Pedretti, J., & Voelker, D. R. (1993). Phosphatidylserine decarboxylase from Saccharomyces cerevisiae. Isolation of mutants, cloning of the gene, and creation of a null allele. _Journal of Biological Chemistry_, _268_, 21416–21424. https://doi.org/10.1016/S0021-9258(19)36940-6

Trotter, P. J., & Voelker, D. R. (1995). Identification of a non-mitochondrial phosphatidylserine decarboxylase activity (PSD2) in the yeast Saccharomyces cerevisiae. _Journal of Biological Chemistry_, _270_, 6062–6070. https://doi.org/10.1074/jbc.270.11.6062

van der Laan, M., Bohnert, M., Wiedemann, N., & Pfanner, N. (2012). Role of MINOS in mitochondrial membrane architecture and biogenesis. _Trends in Cell Biology_, _22_, 185–192. https://doi.org/10.1016/j.tcb.2012.01.004

Vance, J. E., & Steenbergen, R. (2005). Metabolism and functions of phosphatidylserine. _Progress in Lipid Research_, _44_, 207–234. https://doi.org/10.1016/j.plipres.2005.05.001

Vander Heiden, M. G., Chandel, N. S., Li, X. X., Schumacker, P. T., Colombini, M., & Thompson, C. B. (2000). Outer mitochondrial membrane permeability can regulate coupled respiration and cell survival. _Proceedings of the National Academy of Sciences, USA_, _97_, 4666–4671. https://doi.org/10.1073/pnas.090082297

Voelker, D. R. (1997). Phosphatidylserine decarboxylase. _Biochimica et Biophysica Acta (BBA) – Lipids and Lipid Metabolism_, _1348_, 236–244. https://doi.org/10.1016/S0005-2760(97)00101-X

Wadhwa, R., Taira, K., & Kaul, S. C. (2002). An Hsp70 family chaperone, mortalin/mthsp70/PBP74/Grp75: what, when, and where? _Cell Stress and Chaperones_, _7_, 309–316. https://doi.org/10.1379/1466-1268(2002)007<0309:AHFCMM>2.0.CO;2

Waizenegger, T., Stan, T., Neupert, W., & Rapaport, D. (2003). Signal-anchor domains of proteins of the outer membrane of mitochondria: structural and functional characteristics. _Journal of Biological Chemistry_, _278_, 42064–42071. https://doi.org/10.1074/jbc.M305736200

Wenz, L.-S., Opalinski, U., Schuler, M.-H., Ellenrieder, L., Ieva, R., Bottinger, L., Qiu, J., van der Laan, M., Wiedemann, N., Guiard, B., Pfanner, N., & Becker, T. (2014). The presequence pathway is involved in protein sorting to the mitochondrial outer membrane. _EMBO Reports_. _15_, 678–685. https://doi.org/10.1002/embr.201338144

Westermann, B., & Neupert, W. (2000). Mitochondria-targeted green fluorescent proteins: convenient tools for the study of organelle biogenesis in _Saccharomyces cerevisiae_. _Yeast_, _16_, 1421–1427. https://doi.org/10.1002/1097-0061(200011)16:15<1421:AID-YEA624>3.0.CO;2-U

Yaffe, M. P., Jensen, R. E., & Guido, E. C. (1989). The major 45-kDa protein of the yeast mitochondrial outer membrane is not essential for cell growth or mitochondrial function. _Journal of Biological Chemistry_, _264_, 21091–21096. https://doi.org/10.1016/S0021-9258(19)30050-X

Zerbes, R. M., Bohnert, M., Stroud, D. A., von der Malsburg, K., Kram, A., Oeljeklaus, S., Warscheid, B., Becker, T., Wiedemann, N., Veenhuis, M., van der Klei, I. J., Pfanner, N., & van der Laan, M. (2012). Role of MINOS in mitochondrial membrane architecture: cristae morphology and outer membrane interactions differentially depend on mitofilin domains. _Journal of Molecular Biology_, _422_, 183–191. https://doi.org/10.1016/j.jmb.2012.05.004

Zhao, X., Muller, E. G., & Rothstein, R. (1998). A suppressor of two essential checkpoint genes identifies a novel protein that negatively affects dNTP pools. _Molecular Cell_, _2_, 329–340. https://doi.org/10.1016/S1097-2765(00)80277-4

APPENDIX 1

TABLE A1 Library plasmids rescuing the respiratory deficient phenotype of the SPMs

	Chromosome				Growth rescue		
	Number	From	To	Genes on the plasmid	Δom45, gem1 (S324N)	Δom45, gem1 (R103K)	Δom45, ugo1 (P189L)
Isolated from synthetic petite mutant Δom45, gem1 (S324N)							
L	X	204,547	209,,917	MDV1,CCT7	3/3 weak		
L	III	175,407 175,411	178,862 178,866	RPS14A,SNR65SNR189			
L	X	39,879	41,655	NUC1	1/3 weak	1/3 weak	
H	VII	937,532	942,532	**PET54**	3/3 weak	0/3	
	VII	937,396	940,318	**PET54**	3/3 weak	0/3	
L	IV	1,320,450	1,325,454	RPN9,YDR426C,BNA7,TIF35	3/3 weak	3/4 weak	
L	Not sequenced				3/3 weak	3/3 weak	
L	I	50,217 52,050	55,793 55,793	AIM2,**GEM1**	3/3	3/3	3/3
Isolated from synthetic petite mutant Δom45, ugo1 (P189L)							
	II	575,000	595,000	**FZO1**	0/3	0/3	3/3
	IV	1,399,442	1,407,105	**UGO1**	0/3	0/3	3/3
L	II	162,308	167,700	**PET9**	3/3	3/3	3/3
	IX	79,000	99,000	OM45			
	VII	715,554	719,176	YGR111, **SHY1**	3/3	3/3	3/3
	XIV	386,997	392,422	EXBP6,SPC98			
L	IX	309,455	313,798	**TIM44** , RPB3	3/3 weak	0/3	no
	IX	82,000	102,000	OM45			
L		145,655	150,076	**RTT109** , DNM1	NO	3/3 weak	(0/6)
Isolated from synthetic petite mutant Δom45, gem1 (R103K)							
L	VII	932,885	940,245	**PET54** others			
L	VII	937,760	946,051	**PET54** others	3/3	3/3 weak	
L	IX	93,574	97,460	OM45	3/3	3/3	
L	Not sequenced				3/3 weak	4/4 weak	
L	XV	102,337	102,577	Truncation of PAP2	3/3 weak	3/3 weak	
L					3/3 weak	0/3	
L	Not sequenced				3/3 weak	3/3 weak	
H	V	116,587	117,048	URA3	3/3 weak		
H	Not sequenced				3/3 weak	3/3 weak	
H	XV	766,540	767,312	WTM2, **YOR228C**	3/3	2/3	
H	Not sequenced				3/3 weak	1/3 weak	
H	XVI	830,340	834,690	YPR150W,SUE1,URN1,YPR153W	3/3 weak	0/3	
L	V	91,739	97,260	(ECM10) **SSC3**	3/3 weak	7/7 weak	
L	I	52,050	56,140	GEM1	3/3	3/3	
H	IX	94,170	94,363	OM45	2/2	3/3	
L	VI	52,051	56,163	**GEM1**	3/3	3/3	
H	XVI	341,371	341,810	Truncation of GDE1			
L	XVI	341,370	348,068	**YPL109C** , GDE1	3/3	3/3	
L	V	116,676	117,010	URA3	3/3 weak	0/3	
L	IX	307,795	313,463	**TIM44**	3/3	3/3	3/3
L	XI	384,109	390,299	YKL027w, TFA1	0/3	0/3	
L	Not sequenced				3/3 weak	3/3 weak	

For origin of the plasmid: L-Lacroute library, H-HeAl library. The plasmids are presented in the order of mutants found complemented, although eventually suppression was tested in all three mutants. Chromosome number and location are indicated. Since multiple ORFs were present on most of the library plasmids, the underlined genes were confirmed as the rescuing component after subcloning to separate multiple and single copy vectors. Rescue x/y numbers indicate the number of growing clones (x) out of tested (y). "weak" indicate very weak growth of the rescued colonies. Empty fields: Not tested.
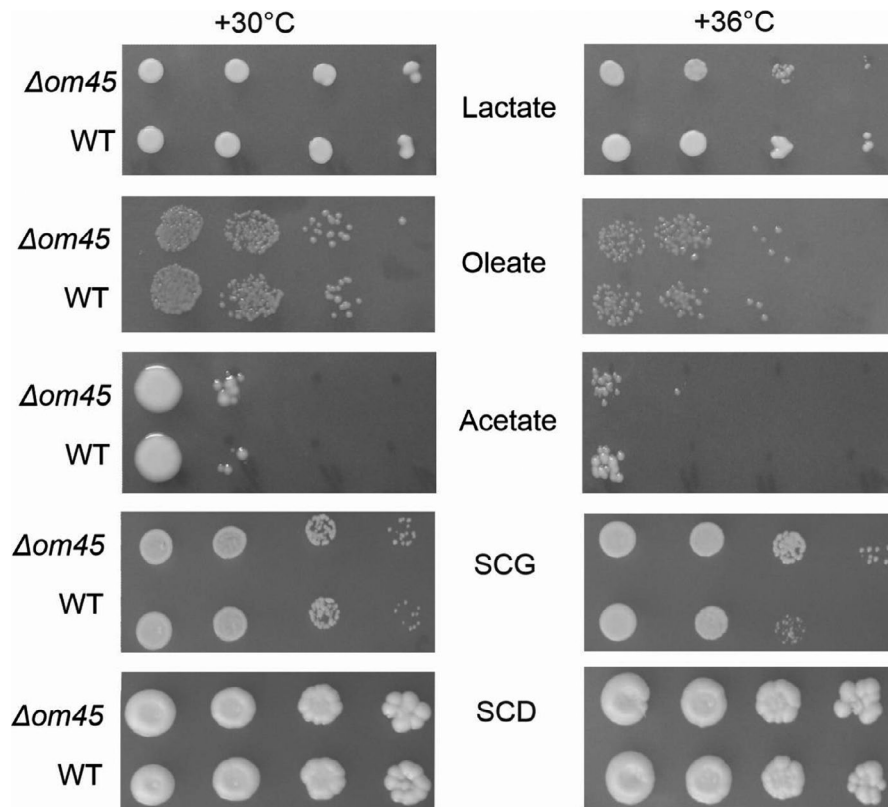
FIGURE A1 Growth phenotype of W1536 8B wild type and om45 deletion strain on different growth media. Yeast strains were grown overnight in SC liquid medium supplemented with glucose. Cultures were normalized to $OD_{595} = 1.0$ and serial 10-fold dilutions were spotted onto corresponding solid media. Photographs were taken after 3–6 days of growth

APPENDIX 2

FIGURE A2 Electron micrographs of W1536 5B-derived WT and rho^0 cells. Panels a–d: W1536 5B cells. Panels c and d are enlarged sections of panels a and b, respectively, as indicated by the boxes in a and b. Panels e–h: W1536 5B rho^0 (Δetr1) cells. Panels g and h are enlarged sections of panels e and f, respectively, as indicated by the boxes in g and h
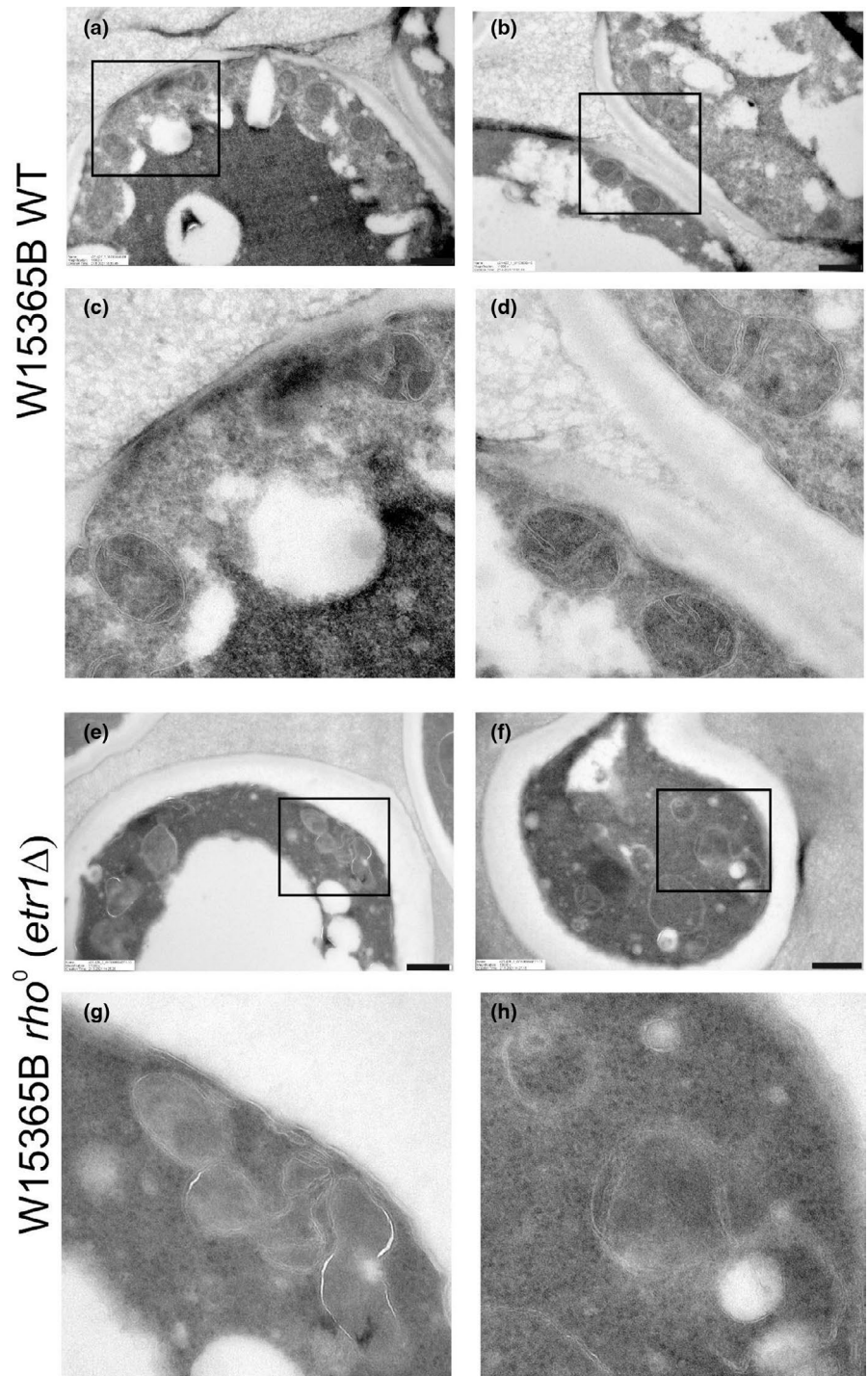
SPM Δom45 ugo1(p189L)
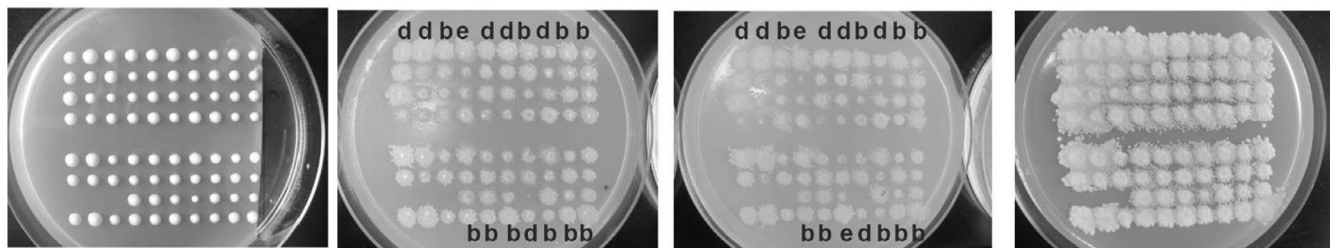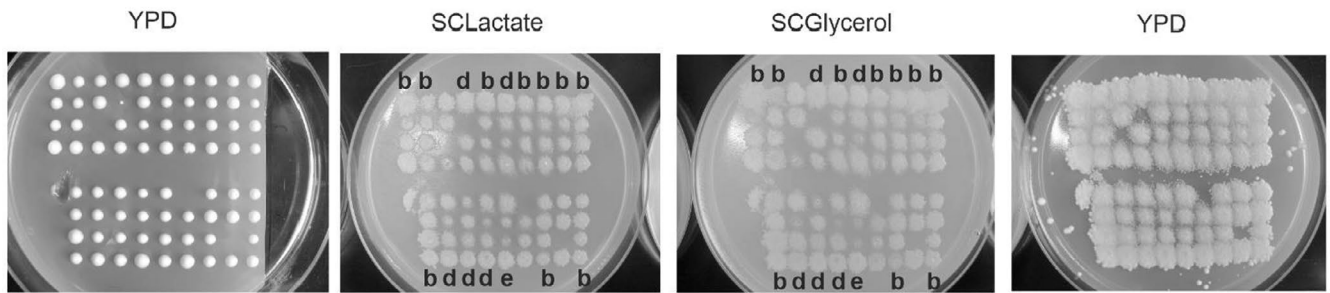
Δom45 gem1(R103K)
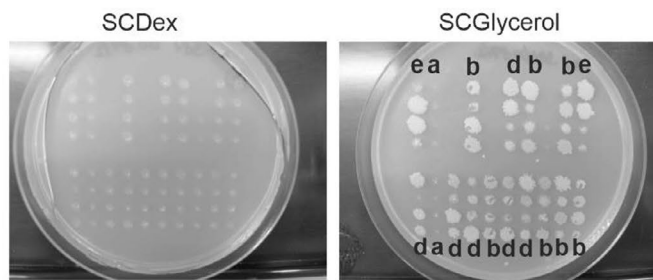
Δom45 gem1(S324N)
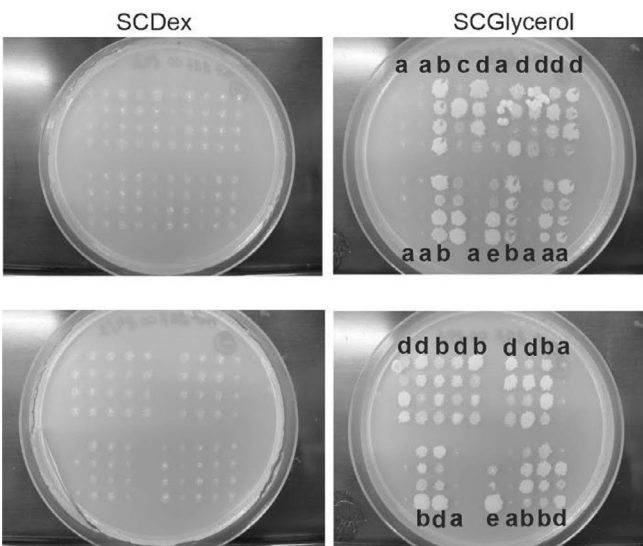
FIGURE A3 Tetrad dissection of SPMs. Cells were initially dissected on YPD or SCD media and then replica plated on the indicated selective media (SCG and SCLac or only SCG). The *Δom45*, *ugo1(P198L)* examples show the dissection master plate before the transfer; the other examples, the SCD master plate AFTER replica plating/transfer. Ratios (respiratory competent: respiratory deficient): a 0:4, b 4:0, c 1:3, d 3:1, e 2:2
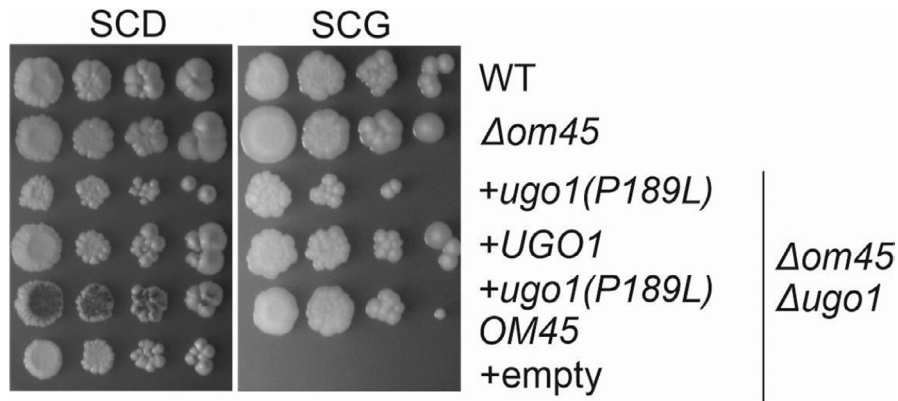
FIGURE A4 Growth of the reconstructed of Δom45/ugo1 SPM. Strains were constructed similarly to the reconstructed *gem1* SPMs (BY series background), initially generating the Δom45, Δugo1 double deletion mutant. However, a plasmid harboring WT *UGO1* was maintained throughout to prevent mitochondrial DNA loss. The reconstructed SPM has a mild growth defect in this strain background, indicating a partial function of the *ugo1(P189L)* – encoded protein. The presence of *UGO1* in the Δom45, Δugo1 mutant completely rescued growth, and the presence of both plasmids carrying the *ugo1(P189L)* mutant allele and *OM45* improved growth compared to the *ugo1(P189L)* construct being present alone, albeit not completely to WT levels on glycerol. When the Δom45, Δugo1 mutant strain only carried empty plasmids, the cells were completely respiratory deficient
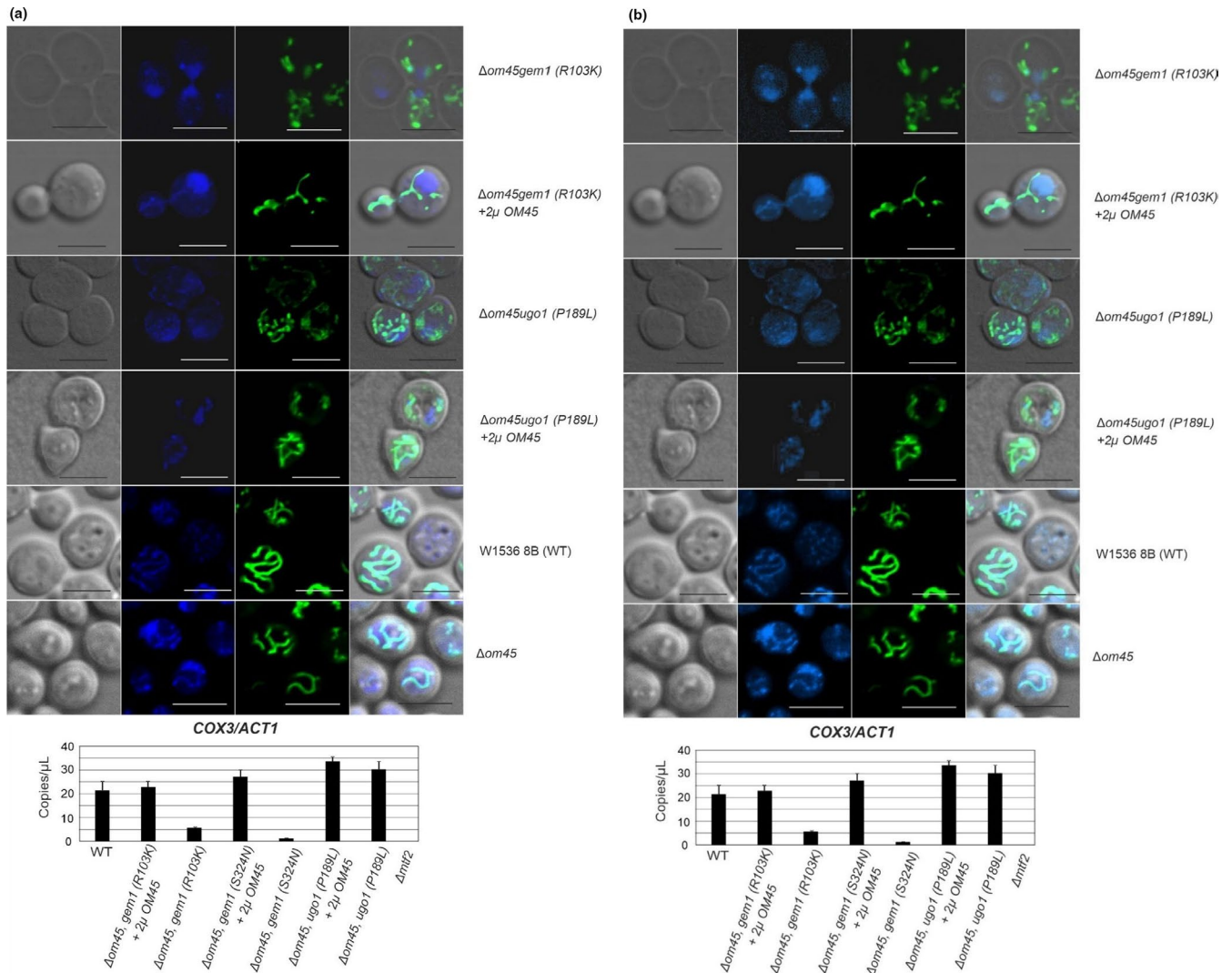
FIGURE A5 Mitochondrial morphology changes and mtDNA loss in the SPM. Representative images of morphology types observed in W1536 8B WT, W1536 8B Δom45, and SPM cells with and without the complementing 2μ OM45 plasmid. Mitochondria visualization was done with matrix targeted mtGFP expressed from plasmid pVT100 U mtGFP(URA3). Cells were grown overnight in a selective liquid synthetic complete medium supplemented with glucose (2%). mtDNA was visualized with a DAPI stain. The concentration of mtDNA was determined with ddPCR in the mutants with and without 2μ OM45 plasmid grown overnight on SC or SC selective medium supplemented with 2% glucose. (a) Original images. (b) same images as in a, but the original blue color of the DAPI stain was replaced with a light turquoise color to enhance the visibility of the DNA stain. (Corel Photo-Paint 2020, 64-bit version, "Replace colors" function in the "Adjust" menu)

FIGURE A6 Growth assay of the W1536 8B Δom45, ugo1(P189L) mutant transformed with multicopy suppressor plasmids

W1536 8B Δom45, gem1 (R103K)
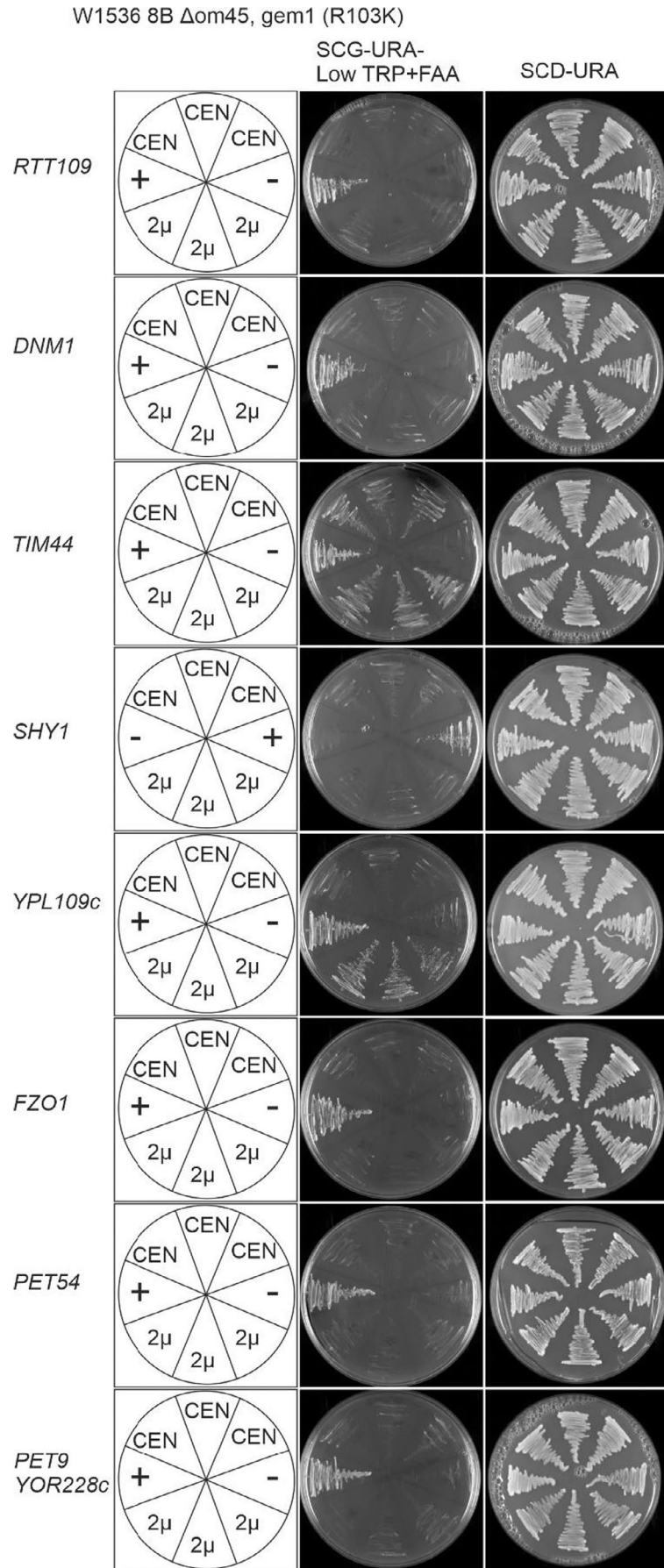
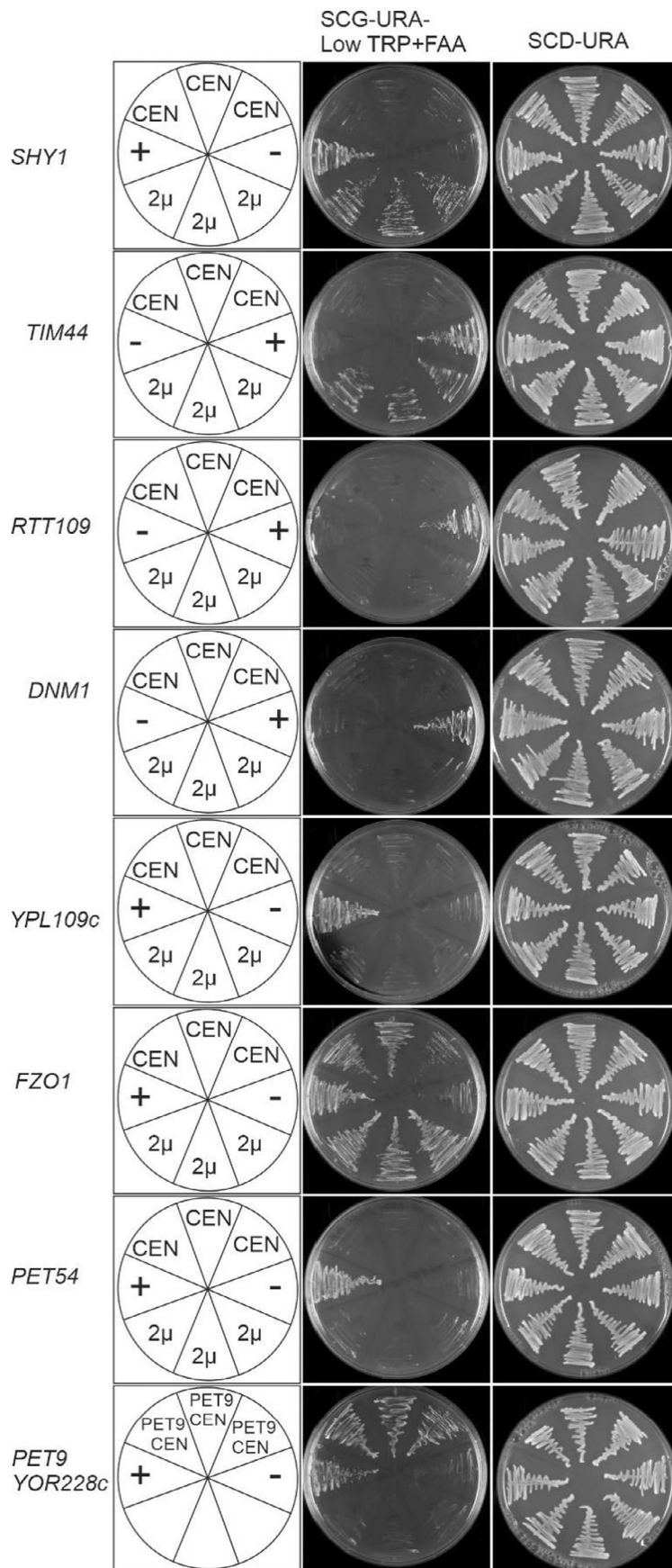W1536 8BΔom45, ugo1 (P189L)

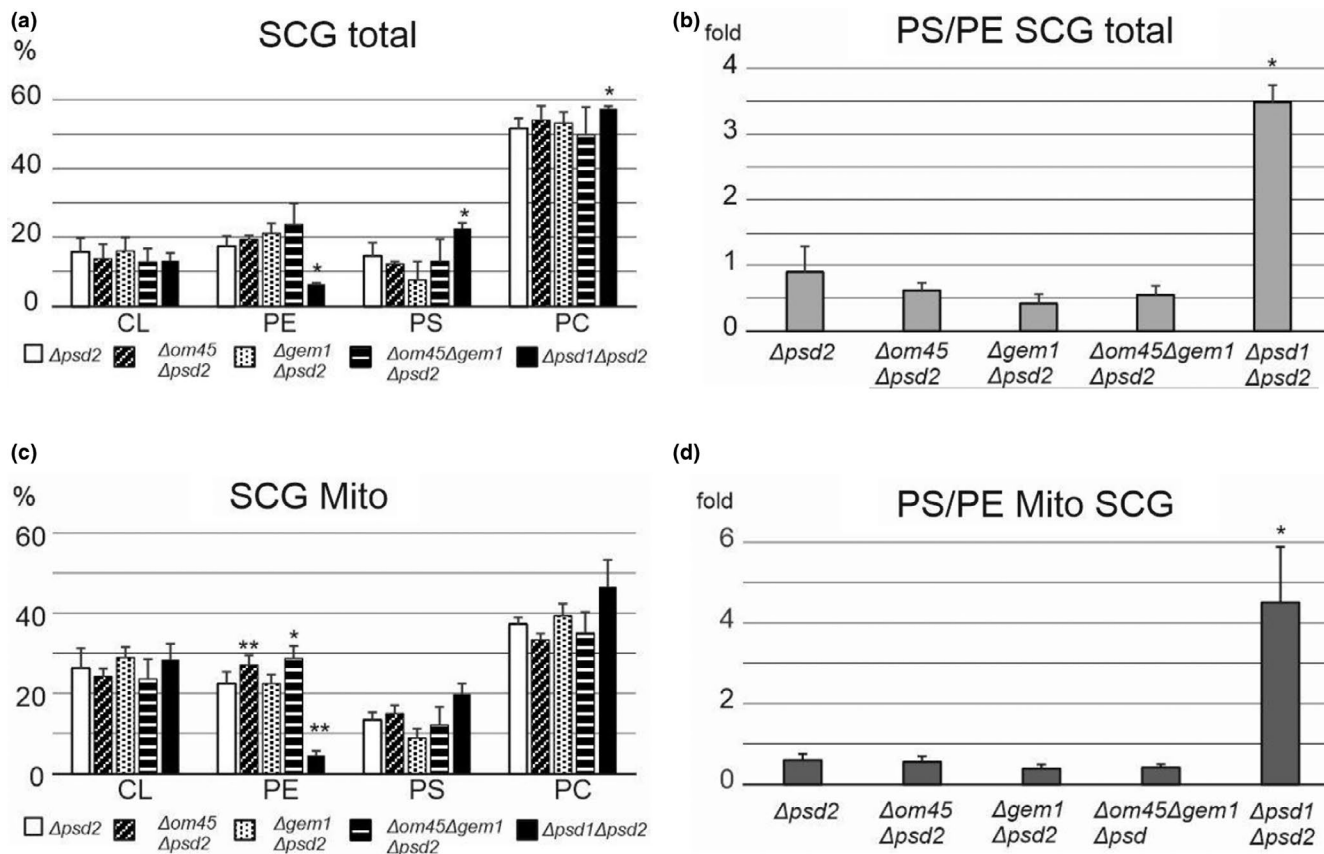**FIGURE A7** Growth assay of the W1536 8BΔom45, gem1(R103K) mutant transformed with multicopy suppressor plasmids

FIGURE A8 Whole cell and mitochondrial phospholipidome analysis of W1536 8B Δpsd2, W1536 8B Δpsd2Δom45, W1536 8B Δpsd2Δgem1, W1536 8BΔpsd2Δom45Δgem1 and W1536 8B Δpsd2Δpsd1 strains. (a) Cellular content of indicated phospholipids from total cells phospholipid preparations in the indicated yeast strains. (b) The ratio of phosphatidylserine over phosphatidylethanolamine from total cell phospholipids. (c) Mitochondrial content of total cells phospholipid preparations in the indicated yeast strains. (d) The ratio of phosphatidylserine over phosphatidyletanolamine from mitochondrial phospholipids preparations. CL, cardiolipin; PE, phosphatidylethanolamine; PS, phosphatidylserine; PC, phosphatidylcholine. Phospholipids were extracted either from whole cells grown on SCG or from mitochondria purified from cells grown on SCG. The pictures present % ratios with the total sample phospholipids set as100%. The statistically supported changes as indicated with * between the samples and W 1536 8B Δpsd2 control ($p < 0.05$), **($p < 0.01$) were determined with a t-test